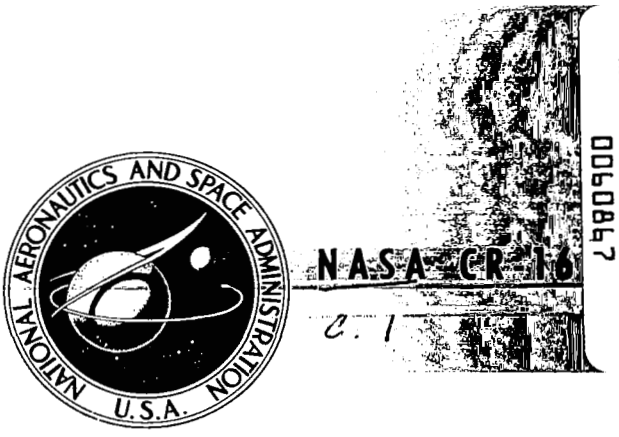

NASA CONTRACTOR REPORT

NASA CR-1673

DESIGN AND FABRICATION OF GALLIUM PHOSPHIDE RECTIFIERS

by Arnold S. Epstein

Prepared by
MONSANTO RESEARCH CORPORATION
St. Louis, Mo. 63166
for

NATIONAL AERONAUTICS AND SPACE ADMINISTRATION • WASHINGTON, D. C. • OCTOBER 1970

1. Report No. NASA CR-1673	2. Government Accession No.	3. Recipient's Catalog No.
4. Title and Subtitle DESIGN AND FABRICATION OF GALLIUM PHOSPHIDE RECTIFIERS		5. Report Date October 1970 6. Performing Organization Code
7. Author(s) Arnold S. Epstein		8. Performing Organization Report No. None
9. Performing Organization Name and Address Monsanto Research Corporation 800 North Lindbergh Boulevard St. Louis, Missouri 63166		10. Work Unit No. 11. Contract or Grant No. NAS 3-12972 13. Type of Report and Period Covered Contractor Report
12. Sponsoring Agency Name and Address National Aeronautics and Space Administration Washington, D.C. 20546		14. Sponsoring Agency Code

15. Supplementary Notes

16. Abstract

High temperature gallium phosphide rectifiers have been designed and fabricated which at 400° C can carry one-half ampere at about three volts. D. C. reverse voltage at 400° C is over 50 volts (75 volts peak inverse) at 5 milliamperes reverse current. The junctions were fabricated using a state of the art technique, namely, closed tube zinc diffusions. The applicability of another fabrication technique, a solid-solid diffusion technique, has been demonstrated. GaP rectifiers with D.C. reverse voltages of 175 volts (240 volts, peak inverse) were obtained at 300° C, while the forward voltage drop noted with a half ampere forward current was 5.7 volts at 300° C. The exact nature of the electrical structure formed has not as yet been determined.

17. Key Words (Suggested by Author(s))	18. Distribution Statement
1. Gallium phosphide 2. High-temperature rectifiers	Unclassified - unlimited

19. Security Classif. (of this report)	20. Security Classif. (of this page)	21. No. of Pages	22. Price*
Unclassified	Unclassified	65	$3.00

*For sale by the Clearinghouse for Federal Scientific and Technical Information
Springfield, Virginia 22151

FOREWORD

The Monsanto Research Corporation performed the work described herein under NASA contract NAS 3-12972 with Mrs. Suzanne T. Weinstein, Direct Energy Conversion Division, NASA Lewis Research Center, as NASA Project Manager.

TABLE OF CONTENTS

TABLE OF CONTENTS (Cont'd)

FIGURES AND FIGURE TITLES

FIGURES AND FIGURE TITLES (Cont'd)

LIST OF TABLES

I. SUMMARY

Half ampere gallium phosphide rectifiers with current densities of 30 ampere/cm^2 have been developed from epitaxially deposited single crystal gallium phosphide. These rectifiers can operate at ambient temperatures of 400°C.

Best overall characteristics at 400°C are a D. C. forward voltage drop of 3 volts (for half ampere current) and a D. C. reverse voltage of 54 volts (~75 volts PIV) at 5ma reverse current. The reverse voltage was somewhat lower than hoped for. These results were obtained by forming p-n junctions using zinc vapor-solid diffusion in a closed tube.

Using another fabrication approach, namely a zinc solid-solid diffusion technique (oxide process) to fabricate GaP rectifiers, we have been able to make a rectifier which operates at 300°C with a D. C. reverse voltage of 175 volts (at 200 microampere reverse current) and a D. C. forward voltage drop of 5.7 volts at 0.5 amperes. The room temperature characteristics were 4.6 volts forward drop at 0.5 amperes and 180 volts D. C. reverse voltage with a reverse current of 100 μa. The exact structure has not been determined or the process optimized; although, if it is a p-n junction, the p layer is very shallow and less than 1/4 micron. We believe that the structure may be of the metal-insulator - (n) semiconductor type. An interesting aspect of the process is that a negative resistance was found in the forward direction.

The single crystal gallium phosphide used to fabricate the rectifiers was n-type with room temperature carrier concentration of mid $10^{16}/cm^3$, liquid nitrogen mobility of about 1200 cm^2/volt-sec and an etch pit density of about 10^6 etch pits/cm . This material was grown on GaAs substrates, primarily on the <111>B orientation. The epitaxial material was of imperfect structure as evidenced by the high dislocation density. Deep level impurities such as oxygen were present, and the existence of vacancies was a distinct possibility. Sulfur and nitrogen seemed to be present. The presence of these impurities and the deep levels prevented the reduction of background carrier concentrations below about 2 to 3 x $10^{16}/cm^3$; as a consequence, reverse voltages of these materials when prepared by standard zinc diffusion were lower than the desired 150 volts PIV.

The presence of a second shallow donor dopant such as tellurium in addition to the sulfur donor appeared to produce material which gave the best overall I-V rectifier characteristics and was the most stable. There was little change in the forward characteristic with temperature up to 400°C.

The housings designed for the rectifiers were adequate to handle the thermal problems.

II. INTRODUCTION

Rectifiers of high current capacity and with a high blocking voltage are required in the kilowatt and megawatt power systems contemplated for aerospace application. These components must be light weight, small size and low power loss; be capable of operating at high ambient temperatures, and be able to withstand a high density nuclear radiation flux.

Many of the devices being used are made of silicon, which imposes an upper temperature limit of 200°C. For high ambient temperature uses, large thermal shielding and cooling facilities are required.

Some work has been done and is being done in developing ceramic tubes for high temperature applications. This approach, however, has its inherent drawbacks because ceramic tubes are bulky and have large power losses.

The requirements for electronic components such as rectifiers and diodes to operate over large temperature ranges, for example between -55°C and 400°C, limits the possible semiconductor materials that can be considered.

Of the candidate materials currently available, only silicon carbide and gallium phosphide meet the requirements of high band gap, chemical stability, and good thermal conductivity. There is great difficulty, however, in growing single crystals of silicon carbide and controlling its purity; thus, of the materials available and suitable for this application, only GaP offers large single crystals with relatively high purity. Davis[1] and Mandelkorn[2] pointed out some years ago the potentialities of GaP as a high temperature rectifier. The ability to fabricate gallium phosphide into junction devices along with the improvement in material purity has increased the interest in the application of gallium phosphide for high temperature rectifiers.

III. RECTIFIER DESIGN

A. MATERIAL

Single crystal gallium phosphide crystals of the order of 2 cm^2 can be epitaxially grown on monocrystalline GaAs or GaP by an open tube vapor transport process. The material can be doped either n- or p-type with moderate control. N-type crystals can be varied in concentration from mid 10^{15} to 10^{18} electrons/cm^3.

B. REVERSE BREAKDOWN VOLTAGE

The breakdown voltage of a p-n junction under ideal conditions is determined by the impurity concentration on the lightly doped side of the junction. Using zinc diffused GaP p-n junctions, we measured the reverse breakdown voltage for various n-type concentrations. The results are shown in Figure 1 together with the calculated values of Sze and Gibbons for an abrupt junction[3]. As can be seen, to obtain D. C. reverse voltages of 100 volts or greater, carrier concentration less than $10^{16}/cm^3$ are required. At these impurity concentrations the depletion region is less than 10 microns at 100 volts reverse.

It is desirable to minimize the rectifier area to obtain maximum breakdown, because the probability of encountering defects increases with the area. However, additional considerations of forward current and thermal resistance also play important roles in determining the area requirements for the rectifier.

C. FORWARD CURRENT CAPACITY

Gallium phosphide, with its large band gap, presents difficulties arising from defects, strain, poor structure, and deep level impurities (which lead to poor lifetime and non-planar junctions) as well as from the presence of carrier compensation through the presence of deep levels. The combination of those effects makes conductivity modulation difficult except where the n-carrier concentration is high ($>10^{17}/cm^3$) but at these values the reverse voltages attainable, according to Figure 1, are of the order of only 20 volts.

Previous work had indicated a current density of about 30 amperes/cm^2 could be achieved without undue difficulties from heating, contacting, etc.[4]. Therefore, an area of about 1.6×10^{-2} cm^2 was needed (chip size 0.127 x 0.127 cm^2) to carry 0.5 amp.

A thickness of 150 microns was selected to minimize strains and stresses due to thermal mismatch without unduly increasing electrical and thermal resistance. To reduce the sheet resistance of the p+ surface, a metallic layer of aluminum was used. An evaporated Ni-Ge-Au layer, carefully heat treated, was used on the n-type side for contact.

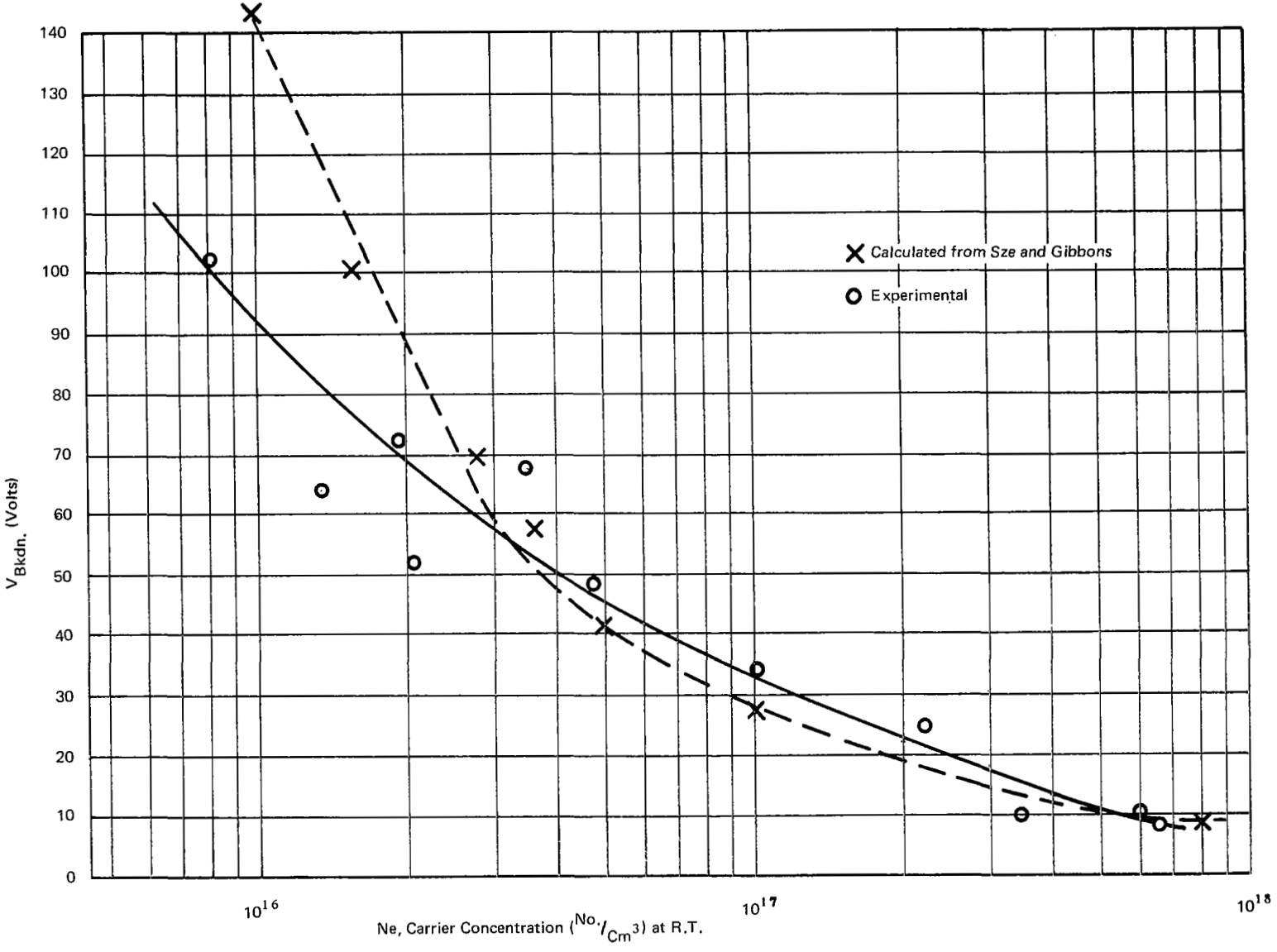

FIGURE 1 REVERSE VOLTAGE BREAKDOWN VS. CARRIER CONCENTRATION FOR n-TYPE GaP

D. THERMAL AND MECHANICAL CONSIDERATIONS IN RECTIFIER DESIGN

GaP has a thermal conductivity of 0.77 watt/cm°C at room temperature. The thermal resistance of a structure consisting of a thin aluminum film deposited on the p-side of a 150 micron GaP wafer containing a p-n junction (p-layer thickness of the order of 15 μm) and coated on the bottom of the n-side with a Au-Ge-Ni contact was calculated to be less than 1.5°C/watt. However, the expected thermal characteristics could be altered by the forward drop increasing with temperature due to the difficulty of injection of minority carriers into the lightly doped material. It was, therefore, desirable to use a housing having a copper base.

The mounting of wafers involves rapid heating and cooling between 20°C and 500°C, and in operation the rectifier will be subject to cycling between 400°C and room temperature or lower. The differences in thermal expansion between the various materials such as GaP and copper, for example, generate stresses in the wafer that must be controlled to prevent fracture failures*. The semiconductor wafer is the most sensitive part of the configuration, and any cracking will result in catastrophic electrical failure. Since the high thermal conductivity of copper (3.93 watt/cm°C) is most desirable in order to remove the heat generated in the GaP wafer, but the expansion mismatch between copper and gallium phosphide would cause fracture of the chip or a pulling of the chip away from the stud, a stress-relief insert between the copper stud and GaP wafer was employed.

The materials considered as stress relief inserts were tungsten, steel, kovar, molybdenum, alloys of (15% Ag, 85% W), (15% Ni, 99.5% W), (9% Cu, 91% W). Of these, molybdenum has a thermal expansion coefficient very close to gallium phosphide, has good thermal conductivity (∿1.4 watts/cm°C) and is readily available. It was, therefore, chosen over the metal-tungsten alloys even though these might be tailored somewhat closer to the expansion coefficient of gallium phosphide.

The molybdenum insert between the GaP and copper stud was .080" x .080" (200 microns x 200 microns) and .005" (125 microns) thick. The molybdenum was gold clad on both sides to insure easy alloying to the GaP and gold clad copper stud. The contact to the p face was made to a thin surface film of aluminum through a series of aluminum wires. With the high thermal conductivity of aluminum and the use of multiple contact wires, the heat was effectively removed from the p-side of the junction.

---

*Another type of stress and strain that has to be considered is that introduced in the material during growth. This cannot be easily controlled and leads to poor junctions, irreversibility and eventual electrical shorting.

E. RECTIFIER AND ENCAPSULATION DESIGN

The rectifier configuration which was selected is shown in Figure 2.

A series of small aluminum wires forming a "spoke" were bonded on one end to the aluminum (p+) gallium phosphide surface. These wires terminated on the periphery of the gold plated Kovar rim of the housing. The rim served as the positive contact. Bonding to these surfaces was accomplished by ultrasonic means. The contact arrangement described above provided assurance of good thermal and electrical conductivity, eased stress on the gallium phosphide, eliminated alignment difficulties, and reduced problems encountered with use of a bulky rigid contact. The arrangement is shown in Figure 3.

The housing (enclosure) configuration, including dimensions and materials, is shown in Figure 4. The housing provided a low thermal resistance and was capable of handling the power dissipation of the diode.

The enclosure, illustrated in Figure 4, utilized alumina as an insulator between the copper stud and the upper rim which was gold plated Kovar. An extension of the rim beyond the actual housing permitted easy access for external contacting of a lead. A nickel (TO-5) can was welded to the Kovar rim thus closing the unit and providing protection for the basic gallium phosphide structure.

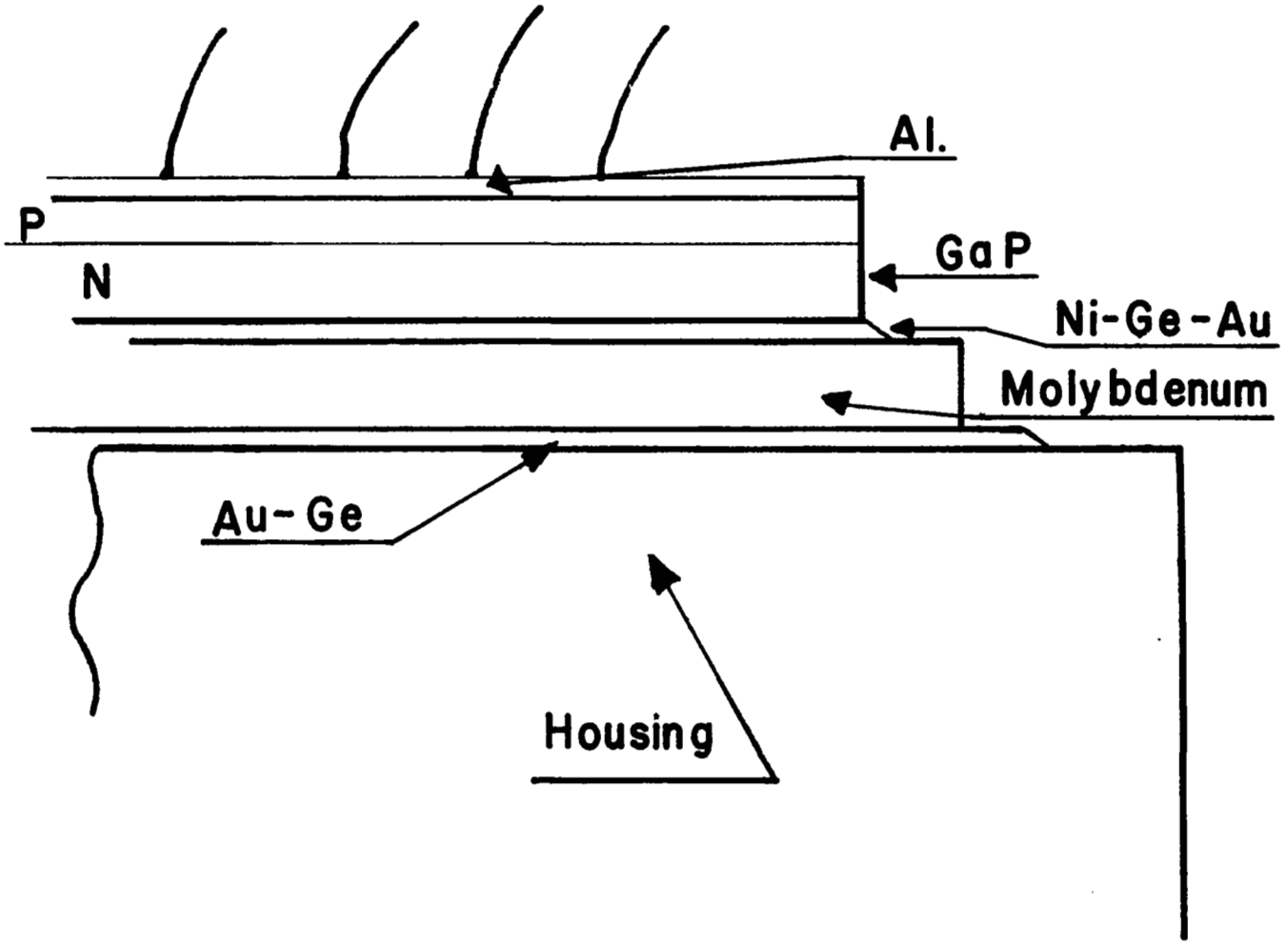

FIGURE 2. DIODE ASSEMBLY

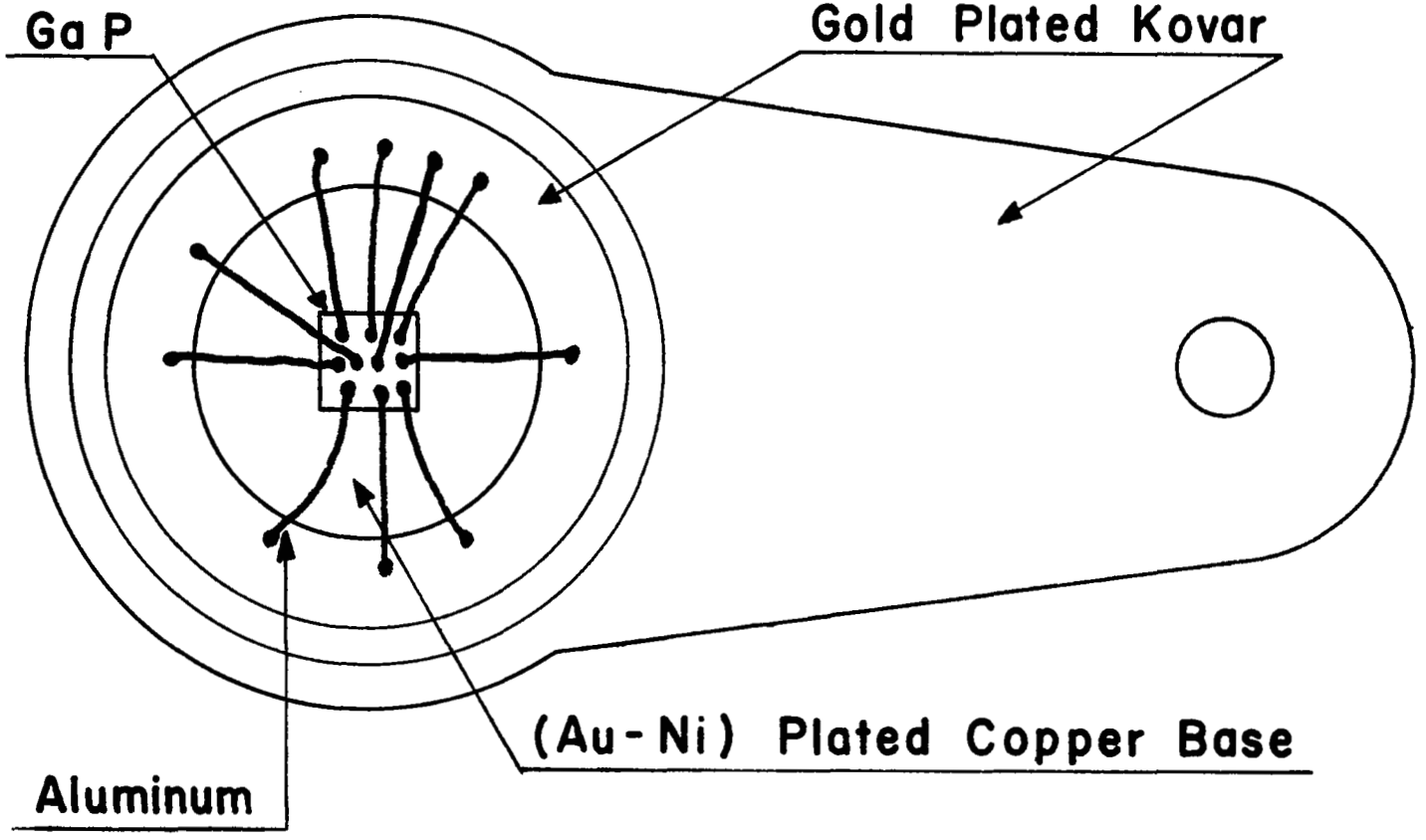

FIGURE 3. SPOKE CONTACT ASSEMBLY

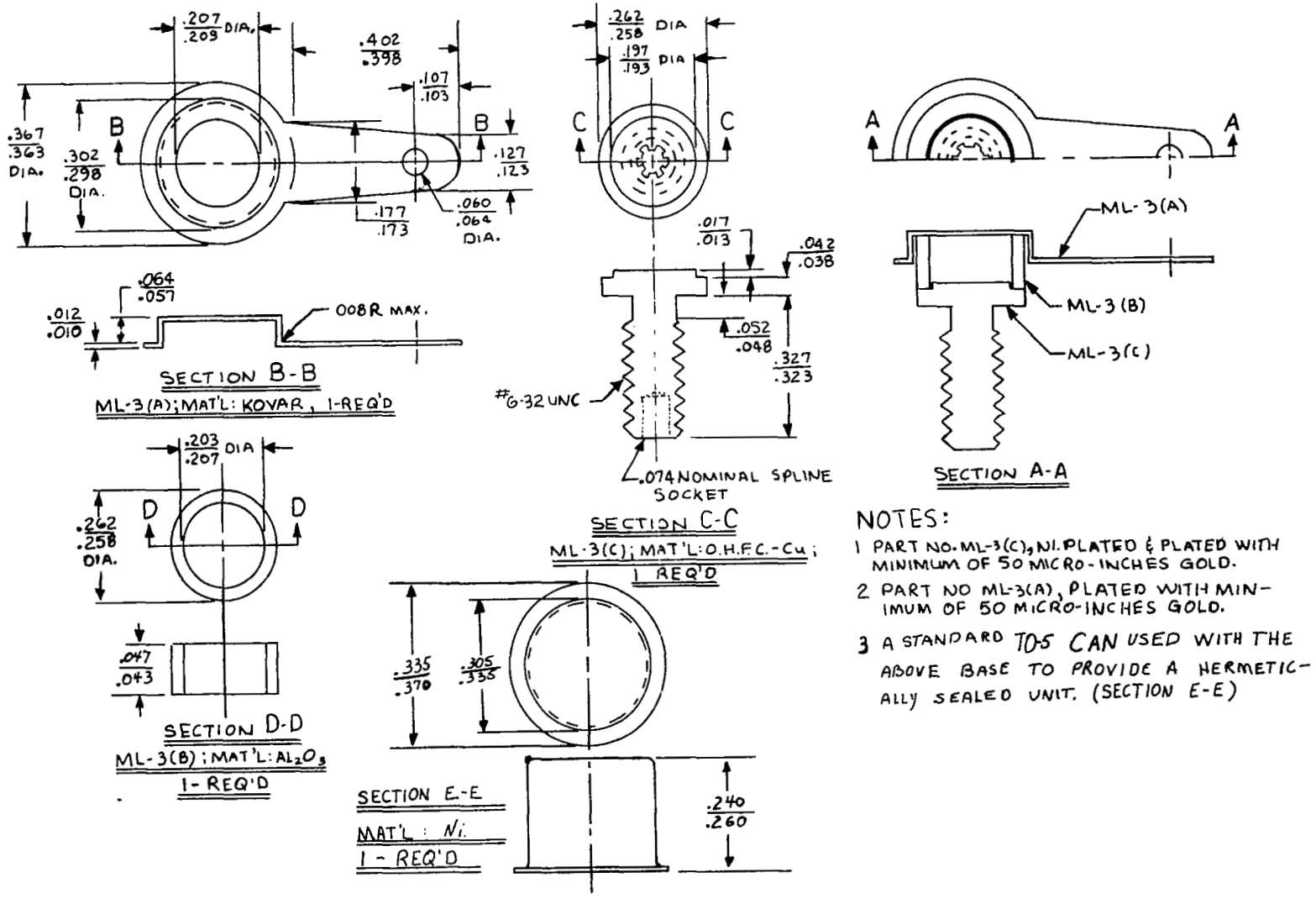

NOTES:

1 PART NO. ML-3(C), NI. PLATED & PLATED WITH MINIMUM OF 50 MICRO-INCHES GOLD.

2 PART NO ML-3(A), PLATED WITH MINIMUM OF 50 MICRO-INCHES GOLD.

3 A STANDARD TO-5 CAN USED WITH THE ABOVE BASE TO PROVIDE A HERMETICALLY SEALED UNIT. (SECTION E-E)

FIGURE 4. HOUSING DESIGN AND CONFIGURATION

IV. MATERIAL PREPARATION AND ANALYSIS

A. CRYSTAL GROWTH

Most of the single crystal gallium phosphide used was prepared by vapor epitaxial deposition on gallium arsenide substrates. The reagents used were anhydrous hydrogen chloride, elemental gallium, phosphine and hydrogen. An open flow system in which quartz was the material in contact with the reactants at high temperatures, was used.

Toward the end of the contract, a few single crystals of GaP were grown using monocrystalline gallium phosphide substrates. Growth was in both the <111>B and <111>A directions.

Slices of gallium phosphide, grown by the liquid encapsulation technique[5], were also made available to us from Metals Research Limited, Melbourn, Royston, Herts, England.

Finally, a grown p-n junction of gallium phosphide was made using zinc as the p dopant.

B. PROPERTIES

1. Orientation

Most of the material grown had <111>B orientation. The <100> grown GaP appeared to have a higher background acceptor concentration than found for the <111>B orientation. As Groves[6] and van der Does de Bye, et. al.[7] have shown, impurity doping is orientation dependent. They have noted, for example, that sulfur may be present by a factor of ten higher in a crystal grown on the <111>B face as on a <111>A face. Conversely the acceptor zinc has a greater affinity for the <111>A face than for the <111>B face. Since an n-type layer was desired the <111>B orientation was favored.

2. Electrical Properties

Table I summarizes the electrical characteristics of the single crystal GaP material obtained on this contract. Included also are the orientation and thickness of each wafer. All of the material was n-type except where noted. The carrier concentration, mobility, and resistivity of each crystal at 300°K and also at liquid nitrogen temperature are given. The room temperature carrier concentrations range from 10^{15} to $10^{18}/cm^3$. The highest 77°K mobility found was about 1500 cm^2/volt-sec. Samples with thicknesses less than 200 microns were generally found to have poor structure. Most of the samples were grown on GaAs substrates. The sample with <111>A orientation had a low carrier concentration, and there was difficulty in making the measurements at 77°K. Samples grown on GaP substrates are also shown as is the grown p-n junction. The lowest free carrier levels achieved for <111>B growth are about 2 x 10^{16}

Table I

ELECTRICAL CHARACTERISTICS OF n-TYPE GaP CRYSTALS GROWN

Sample	Orientation	How Grown	Thickness (Microns)	Carrier Concentration N_e (no/cm^3)	Electron Mobility μ(cm^2/volt sec.)	Resistivity ρ (ohm cm)	Temperature of Measurement ($^\circ$K)
GP 1-4-1	<111> B	Vapor Epitaxial GaAs Substrate	191	3.6×10^{17} 3.6×10^{14}	100 525	0.17 33	300 77
GP 1-4-2	<111> B	"	117	2.7×10^{17} 2.2×10^{14}	121 959	0.18 3.0	300 77
GP 1-4-3	<111> B	"	106	1.57×10^{17} 1.09×10^{14}	116 1033	0.34 55	300 77
GP 1-5-1	<111> B	"	92	1.9×10^{18} 5.3×10^{15}	72 139	0.04 8.4	300 77
GP 1-5-2	<111> B	"	110	1.53×10^{17} 1.55×10^{14}	134 964	0.30 42	300 77
G 20-38	<111> B	"	156	2.5×10^{17} 9.1×10^{14}	161 1200	0.15 5.7	300 77
G 20-39	<111> B	"	453	6.4×10^{16} 2.5×10^{14}	182 1470	0.54 17.0	300 77
G 20-41	<111> B	"	428	6.8×10^{16} 2.9×10^{14}	189 1169	0.48 18.2	300 77
G 20-42	<111> B	"	272	5.6×10^{16} 1.47×10^{14}	188 1048	0.60 41	300 77
2-358-3	<100>	"	271	4.3×10^{16} 1.13×10^{14}	173 1535	0.83 36.0	300 77
029	<111> B	Liquid Encapsulation	375	2.5×10^{17} 4.3×10^{13}	105 330	0.23 446	300 77
GP 1-1-2	<111> B	Vapor Epitaxial GaAs Substrate	112	2.6×10^{17} 1.05×10^{14}	117 1000	0.21 59	300 77
G 21-28-2	<111> B	Vapor Epitaxial	412	3.7×10^{16} 1.30×10^{14}	127 1106	1.34 43	300 77
G 21-28-1	<100>	"	-	high p, could not measure -	- -	- -	- -
GP 2-2-1	<100>	"	118	1.76×10^{16} 6.1×10^{13}	133 1083	2.70 94	300 77
GP 2-2-2	<111> B	"	176	1.15×10^{17} 2.1×10^{14}	134 1352	0.40 22	300 77
G 21-29-1	<111> B	"	363	3.4×10^{16} 7.3×10^{13}	131 1054	1.40 81	300 77

Table I (cont'd)

ELECTRICAL CHARACTERISTICS OF n-TYPE GaP CRYSTALS GROWN

Sample	Orientation	How Grown	Thickness (Microns)	Carrier Concentration N_e (no/cm^3)	Electron Mobility μ(cm^2/volt sec.)	Resistivity ρ (ohm cm)	Temperature of Measurement ($^\circ$K)
G 21-29-2	<111> B	Vapor Epitaxial	274	5.0×10^{16} 3.5×10^{12}	136 864	0.91 2080	300 77
G 21-29-3	<111> B	"	142	2.4×10^{16} 1.33×10^{13}	94 488	2.70 960	300 77
GP 2-3-1	<111> B	"	366	4.3×10^{17} 4.5×10^{14}	96 441	0.15 31	300 77
GP 2-3-2	<111> B	"	580	4.7×10^{17} -	86 -	0.15 -	300 77
G 21-30-1	<111> B	"	503	5.6×10^{16} 7.7×10^{13}	138 1005	0.81 81	300 77
G 21-30-2	<111> B	"	538	3.1×10^{16} 1.82×10^{13}	123 676	1.65 508	300 77
G 21-30-3	<111> B	"	534	1.67×10^{16} 1.58×10^{13}	129 690	2.90 570	300 77
GP 1-1-2	<111> B	"	112	2.6×10^{17} 1.05×10^{14}	117 1000	0.21 59	300 77
GP 1-1-1	<111> B	"	~150	- -	- -	- -	300 77
GP 1-2-1	<111> B	"	169	3.4×10^{17} 1.66×10^{14}	116 990	0.16 38	300 77
GP 1-2-2	<111> B	"	205	1.15×10^{17} 7.0×10^{13}	124 1250	0.44 72	300 77
GP 1-3-1	<111> B	"	257	2.1×10^{17} 1.55×10^{14}	121 1020	0.24 40	300 77
GP 1-3-2	<111> B	"	161	1.23×10^{17} 7.3×10^{13}	143 1245	0.36 68	300 77
G 20-40	<111> B	"	300	3.6×10^{16} 8.5×10^{13}	193 1100	0.89 67	300 77
GP 2-1	<111> B	"		3.9×10^{17} 4.0×10^{14}	112 482	0.14 0.32	300 77

Table I (cont'd)

ELECTRICAL CHARACTERISTICS OF n-TYPE GaP CRYSTALS GROWN

Sample	Orientation	How Grown	Thickness (Microns)	Carrier Concentration N_e (no/cm^3)	Electron Mobility μ(cm^2/volt sec.)	Resistivity ρ (ohm cm)	Temperature of Measurement (°K)
1	<111> B	Liquid Encapsulation	from ingot	8.6×10^{15}	132	5.50	300
GP 2-4-1	<111> B	Vapor Epitaxial GaAs Substrate	487	2.3×10^{17} 4.2×10^{14}	123 914	0.22 16.2	300 77
GP 2-4-2	<111> B	"	780	5.4×10^{17} 3.0×10^{14}	105 923	0.11 25	300 77
GP 2-4-3	<111> B	Vapor Epitaxial GaAs Substrate	593	1.6×10^{17} 2.3×10^{14}	119 832	0.32 29	300 77
GP 2-5-1	<111> B	"	515	2.4×10^{17} 3.2×10^{14}	134 1037	0.20 18.7	300 77
GP 3-1	<100>	"	132	1.68×10^{15} -	180 -	20.00 -	300 -
GP 3-2-1	<111> B	"	533	5.3×10^{17} 3.4×10^{14}	129 940	0.09 20	300 77
GP 3-2-2	<111> A	"	500	1.6×10^{15} -	101 -	39.00 -	300 77
Grown p-n junction		"	p layer 20-25 microns n-layer 320-560 microns	$P_n = 9 \times 10^{17}$ $N_e = 1 \times 10^{17}$			300
GP 3-3-1	<111> B	Vapor epitaxial grown on epitaxial GaP substrate	430	5.6×10^{17} 3.0×10^{14}	127 991	0.08 21	300 77
GP 3-3-1	<111> A	"	220	1.45×10^{16}	156 Too high to measure	2.75	300 77
GP 3-3-2	<111> B	Vapor epitaxial grown on bulk GaP substrate	265	3.4×10^{17} 2.8×10^{14}	118 1274	0.15 18	300 77
GP 3-3-2	<111> A	"	280	Unable to measure	- -	- -	300 77

carriers per cm^3 with mobilities at 77°K of about 1500 cm^2/volt-sec. Lower free carrier concentrations obtained on this or other orientations are believed to be due to higher concentrations of deep acceptor impurities or defects.

This background impurity level, whether due to chemical impurities or native defects, was controlled to a large extent by substrate material and orientation, deposition temperature, growth rate, and reactant gas composition. Lattice and thermal expansion mismatch between gallium phosphide and gallium arsenide produces dislocations and strain which are unavoidable when gallium arsenide is used as the substrate.

3. Dislocation Density

Dislocation densities on a number of the wafers grown on GaAs substrates were measured and found to be between $7 \times 10^5/cm^2$ and $7 \times 10^6/cm^2$. The delineation etch was a 1:7::HF:HNO_3 etch with 0.25g of $AgNO_3$ added per 100 cm^3. By contrast the dislocation densities of GaP grown on GaP substrates were considerably lower, being about $6 \times 10^4/cm^2$, of the same order as in bulk pulled GaP crystals.

The effect of dislocation densities on the electrical properties was demonstrated by its effect on the 77°K electron mobility of samples with the lowest impurity concentrations (and highest mobilities). Figure 5 illustrates the role that dislocations can play in affecting the liquid nitrogen mobility. (Because the electron mobility at 77°K is more sensitive to impurities, defects, etc., it has been chosen as a measure of overall crystal quality). It can be seriously affected by an increase in etch pit density. Looked at another way, if the etch pit density can be reduced from 10^6 to 10^5, then the highest mobility obtained can be increased to values above 2000 cm^2/volt-sec at 77°K. Families of curves shown in Figure 5 are for cases where the effect of impurities is greater. With more impurities the number of dislocations required to greatly affect the mobility becomes progressively greater and in some cases densities approaching $10^7/cm^2$ are necessary. At that level the mobility is already too low because of the high impurity concentration and the effect of dislocations is not as apparent.

4. Impurities by Mass Spectrometric Analysis

It is very difficult to find a suitable method, having sufficiently low limits of detection of impurities, for the analysis of GaP. The best results, with respect to the detection limits of critical impurities were obtained by Mass Spectrometry.

Data for some of the more promising GaP samples analyzed by Mass Spectrometry are shown in Table II. Basic impurities detected are oxygen, nitrogen, sulfur and silicon. Corroboration on detection of nitrogen and sulfur in the samples was found with photoluminescence measurements (at liquid helium temperatures). Oxygen was believed to be a residual impurity in the GaP, present as a result of the growing technique.

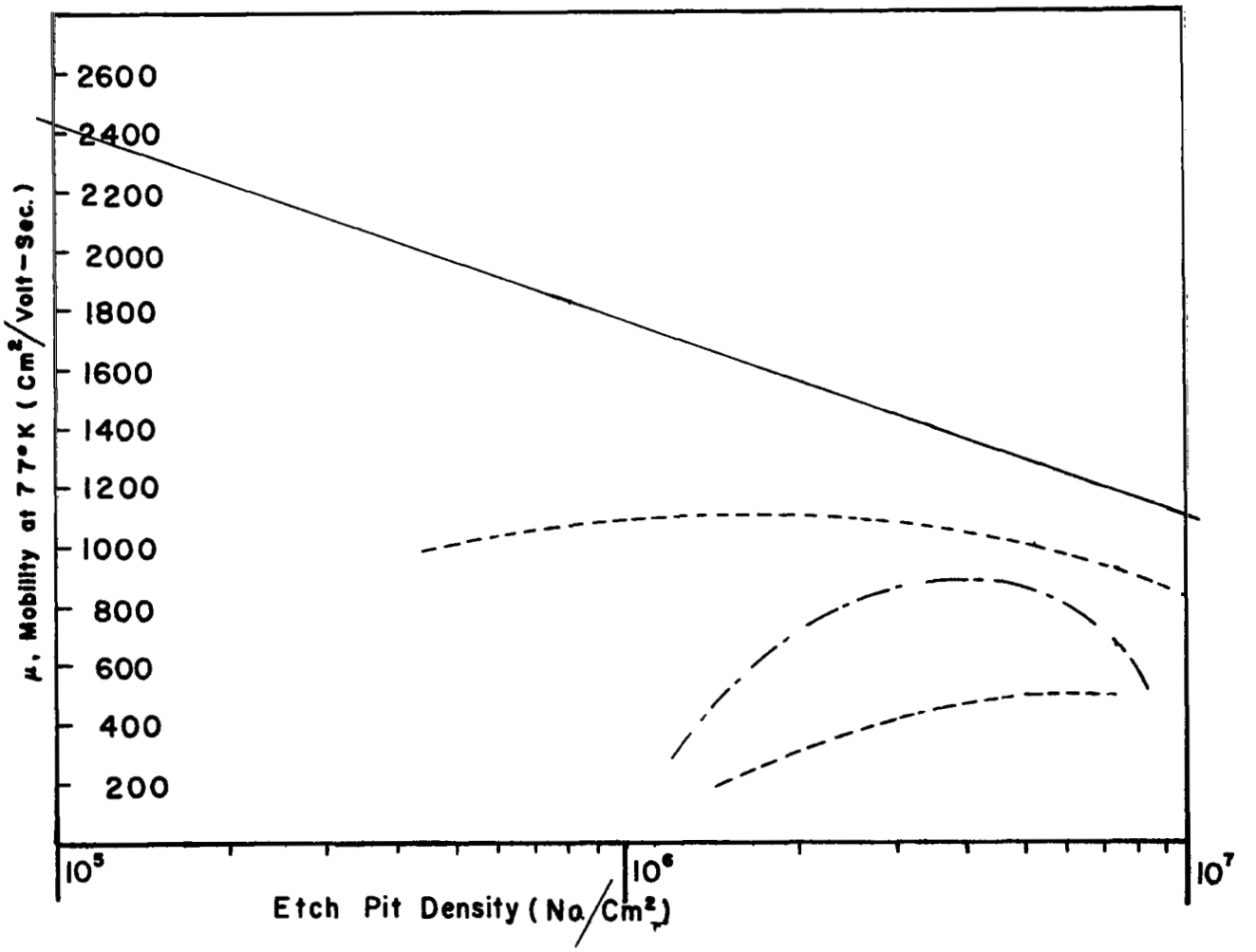

FIGURE 5. ELECTRON MOBILITY AT 77 °K vs ETCH PIT DENSITY

Table II

MASS SPECTROMETER ANALYSIS OF GaP CRYSTALS
GaP SAMPLES

Impurity	GP 1-1-2	G 20-38	G 20-39	G 20-41	G 20-42	2-358-3	029	G 20-40	GP 1-4-1	GP 1-4-2
Carbon	1.40	4.1 - 7.1	2.0 - 3.4	2.20	1.40	0.56	0.72	1.20	1.00	0.70
Nitrogen	0.03	0.30	0.10	1.50	5.20	0.04	0.12	0.05	1.10	0.04
Oxygen	0.70	3.20	1.60	1.60	0.54	0.44	2.50	0.60	0.30	0.20
Silicon	0.20	N.D.	N.D.	~0.10	<<0.10	0.16	<0.10	0.20	0.70	0.20
Sulfur	4.40	~1.50	<1.50	1.10	0.80	0.03	3.50	1.50	~0.30	~0.30
Aluminum	N.D.	0.26	0.14	0.50	0.12	0.24	0.30	0.70	0.09	0.13
Potassium	2.00	4.20	1.10	0.36	0.18	0.05	0.08	0.40	6.00	4.40
Iron	N.D.	N.D.	N.D.	N.D.	N.D.	N.D.	-	N.D.	0.06	0.04
Copper	N.D.	N.D.	0.30	N.D.	N.D.	N.D.	0.05	N.D.	N.D.	N.D.
Magnesium	N.D.	-	-	N.D.	N.D.	N.D.	-	-	N.D.	N.D.
Chlorine	N.D.	N.D.	N.D.	N.D.	N.D.	N.D.	-	N.D.	N.D.	N.D.
Calcium	N.D.	0.18	0.06	0.04	N.D.	N.D.	-	0.06	0.04	0.04
Selenium	N.D.	N.D.	N.D.	N.D.	N.D.	N.D.	-	N.D.	N.D.	N.D.
Tellurium	N.D.	3.10	N.D.	2.10	0.30	N.D.	-	N.D.	N.D.	N.D.
Boron	N.D.	N.D.	N.D.	N.D.	N.D.	N.D.	1.70	N.D.	N.D.	N.D.
Tin	N.D.	-	-	N.D.	N.D.	N.D.	-	N.D.	N.D.	N.D.
Zinc	-	-	-	-	-	-	-	-	N.D.	N.D.
Chromium	-	-	-	-	-	-	-	-	0.34	0.14

NOTE

Impurities in Table above are given in ppma, parts per million atomic. To convert to number of atoms/cm^3 multiply numbers in table by 5×10^{16}. N.D. means impurity looked for but was not detected.

Table II (cont'd)
MASS SPECTROMETER ANALYSIS OF GaP CRYSTALS
GaP SAMPLES

Impurity	GP 1-5-2	GP 2-1	GP 2-3-2	G 21-29-1	G 21-28-2	GP 2-2-2	GP 2-2-1	G 21-29-2	GP 2-4-2
Carbon	1.70	1.70	11.00	3.00	1.30	1.80	6.00	6.60	2.80
Nitrogen	~0.02	~0.02	<0.05	<0.10	<0.01	<0.05	0.05	0.40	-
Oxygen	0.44	1.20	1.60	1.00	0.40	0.40	0.80	1.10	24.00
Silicon	1.70	2.20	6.60	1.00	<1.00	0.24	0.56	0.30	32.00
Sulfur	~0.10	0.20	9.00	<0.17	<0.03	2.80	0.80	0.17	16.00
Aluminum	0.05	0.04	0.40	0.04	<0.03	0.12	0.26	0.03	<0.01
Potassium	3.00	3.20	0.50	0.26	0.06	0.26	0.80	0.12	0.05
Iron	0.03	0.16	0.05	0.05	N.D.	N.D.	N.D.	0.01	0.05
Copper	N.D.	N.D.	N.D.	N.D.	N.D.	N.D.	N.D.	N.D.	0.24
Magnesium	N.D.	N.D.	N.D.	N.D.	N.D.	N.D.	N.D.	N.D.	N.D.
Chlorine	N.D.	N.D.	N.D.	N.D.	N.D.	N.D.	N.D.	N.D.	N.D.
Calcium	0.03	0.04	N.D.	N.D.	N.D.	N.D.	N.D.	N.D.	N.D.
Selenium	N.D.	N.D.	N.D.	N.D.	N.D.	N.D.	N.D.	N.D.	N.D.
Tellurium	N.D.	N.D.	N.D.	N.D.	N.D.	N.D.	N.D.	N.D.	N.D.
Boron	N.D.	N.D.	N.D.	N.D.	N.D.	N.D.	N.D.	N.D.	N.D.
Tin	N.D.	N.D.	N.D.	N.D.	N.D.	N.D.	N.D.	N.D.	N.D.
Zinc	N.D.	N.D.	N.D.	N.D.	N.D.	N.D.	N.D.	N.D.	N.D.
Chromium	0.07	0.02	N.D.	N.D.	N.D.	N.D.	N.D.	N.D.	0.01

NOTE

Impurities in Table above are given in ppma, parts per million atomic. To convert to number of atoms/cm^3 multiply numbers in table by 5×10^{16}. N.D. means impurity looked for but was not detected.

Lowest concentration of oxygen detected was about 0.2 parts per million atomic (1×10^{16} atoms/cm^3). Nitrogen is a background impurity which can be reduced to levels considerably below oxygen. In some samples, example G20-42, it was added during growth using an ammonia source.

The detection of carbon in the samples may indicate its presence as an acceptor or complex or both. It is believed that not all of the carbon goes in as an acceptor. The significance of potassium, magnesium, chlorine and calcium in the GaP has not been established. The better samples were noted to have relatively low amounts of these impurities.

The purest samples were also the samples with the highest mobilities. Samples G20-39 and G20-40 were low in the donor impurities (sulfur, silicon). An interesting sample was G20-41 which had a small concentration of tellurium as well as of sulfur. Rectifiers made from it had some interesting forward characteristics.

While the arsenic content has not been indicated, some arsenic was present in all of the samples grown epitaxially where GaAs was used as a substrate. The amount varied but was generally less than 1%. Vacancies are not detectable but are believed to play a role also.

Sample #029 was grown by the liquid encapsulation technique and, aside from oxygen and sulfur, is quite pure. Boron appears because boric oxide is used as the encapsulant in the growth of the crystal.

Sample 2-358-3 was grown in the <100> orientation. While the relative amounts of impurities detected were low (sulfur $\approx$ 0.03 ppma) it is believed there are additional acceptor levels present (possibly vacancies) along with poor structure leading to poor rectifier characteristics. The correlation between carrier concentration, as deduced from electrical measurements, and the above mass spectrometer data is generally not good. Best correlation was observed for samples GP1-1-2, G20-38, G20-39, G20-42 and GP1-5-2.

Correlations between carbon, oxygen, nitrogen and donors, sulfur, silicon, tellurium, tin and selenium provide indications for usefulness of the material for rectifiers. This will be shown in a later section. (Section V)

The carbon and oxygen contents in the <111>B epitaxially grown crystals follow in almost direct proportions to each other i.e., when the carbon content was high, so was the oxygen. Sample 2-358-3 was grown in the <100> orientation and while the ratio holds, the amounts of these impurities were considerably reduced. Sample #029 grown from the melt shows a considerably larger oxygen than carbon content and inverts the ratio. Sample G20-42 was grown under considerable NH_3 flow rate and oxygen content appeared reduced compared to the carbon level, but the

nitrogen level was considerably greater than for all the other samples. The silicon levels were low in all the samples shown. The prime donor impurities were sulfur and tellurium. The likely acceptor impurity is thought to be carbon; although, the degree to which it behaves as an acceptor is unknown.

5. Photoluminescence

Photoluminescence spectra of GaP at liquid helium temperature have been shown by a number of workers, such as Dean[8], to give rise to sharp emission peaks which can be interpreted in terms of impurities present in the material and in the recognition of strain in the crystal. Data taken on our samples and interpretated according to Ref. 8 indicated the presence of sulfur and nitrogen in all of the samples which was in qualitative agreement with Mass Spectrometer measurements. Least amount of strain was found for GaP crystals grown on GaP substrates in agreement with etch pit measurements. On those samples grown on GaAs substrates, sometimes up to 1% arsenic was reported (deduced from the shift in luminescence peaks). Samples grown in the <111>B or <111>A orientation gave rise to much greater peak emission amplitudes than found for the <100> orientated GaP.

V. RECTIFIER FABRICATION

A. JUNCTION FORMATION

Three different approaches were used to fabricate electrical structures for use as GaP rectifiers. The approaches were zinc diffused from the vapor in a closed tube, a solid-solid diffusion process, and grown p-n junctions using zinc as the p-dopant.

1. Closed Tube Zinc Vapor Diffusion

The most common technique of forming a p-n junction by diffusion of zinc into n type GaP is by sealing the sample with zinc and phosphorous in a closed tube and diffusing at high temperatures for a period of time. This technique was optimized in terms of minimum forward drop at 0.5 amperes (for a given junction area $\approx 1.6 \times 10^{-2}$ cm^2). As long diffusion times tend to provide large gradients and in addition, may lead to thermal etching of the sample, the diffusion times were held to one hour. Forward voltage drops at 0.5 amperes at room temperature for various diffusion temperatures are shown in Table III. The most consistent results and lowest forward drops were obtained at a temperature of 875°C.

The junctions fabricated by this technique were extremely sensitive to poor structure since the zinc diffusion follows defects and fault lines. Consequently, non-planar junctions and junction shorting can result with manifestation of poor and often unstable reverse and forward electrical characteristics.

2. Solid-Solid Diffusion

A second fabrication technique introduced to permit better control of the surface concentration and lessen dependence on bulk defect structure was the solid-solid diffusion process:

The process consists of fabricating the GaP crystal by sequentially depositing and heat treating a plurality of doped and undoped oxide layers on the GaP wafer to form the junction by solid-solid diffusion. The oxide layers are then removed by etching and standard rectifier fabrication processing continued.

One of the most interesting results found using this technique was noted for sample NA79G20-41. We observed a negative resistance in the forward direction which had the effect of reducing the forward drop at high currents, and a D. C. reverse breakdown of 180 volts at room temperature. The latter effect was over four times higher than that for a p-n junction formed by closed tube zinc diffusions discussed in V(A-1) above. The electrical characterization will be discussed further in Section VI on testing and analysis.

Table III

FORWARD VOLTAGE DROP
(V_f AT .5 AMP AT R.T.) VS. ZINC DIFFUSION TEMPERATURE

	Temperature		
Material	800°C	875°C	950°C
G20-38	3.20	2.54	-
G20-39	4.40	7.86	4.31
G20-40	-	4.60	50.00
G20-41	4.10	3.00	3.20
G20-42	4.40	3.42	3.66
029	-	2.10	19.50
GP1-4-2	-	3.25	2.20
GP1-4-1	-	2.58	-

3. Grown Junctions

An attempt was made to grow p-n junctions of GaP from the vapor by depositing on GaAs substrates. The n layer was undoped except for background impurities. The layer thicknesses and concentrations were:

p layer	thickness = 20-25μm concentration = $9 \times 10^{17}/cm^3$
n layer	thickness = 320 - 560μm concentration = $1 \times 10^{17}/cm^3$

The units tested had low reverse breakdowns of ∿20 volts and high forwards of ∿20 volts at 100μa. The results were not attractive enough to warrant further work at this time. The results on the rectifiers will be shown in the section on Test and Analysis (Section VI).

B. CONTACTS

A series of films were investigated for use on the p layer to help in reducing sheet resistance and aid in providing a more uniform contact. Best results were achieved with silver and aluminum. Since aluminum wire was used to make contact between the p layer and the positive contact on the housing, it was felt that use of the aluminum film would reduce the possibility of undesirable alloying effects between different metals (such as between silver and aluminum) which might result because of the high temperature operation of the rectifier. A film thickness of about 1 micron was used.

For the n type contact (GaAs substrate having been removed) a film of germanium-nickel-gold was evaporated on the n side and was alloyed with a gold-germanium preform to a gold clad molybdenum sheet. The gold-molybdenum sheet was alloyed to the header by a gold-germanium alloy. The whole alloying operation was carried out at 500°C.

C. JUNCTION ISOLATION

An etch for the GaP junction region had to be selected that was moderate and would not attack some of the more reactive elements such as aluminum or the housing. To etch the junction, an etching solution consisting of 80% ($3H_2SO_4$: $1H_2O$) and 20% H_2O_2 was selected. The etch was heated to 50°C. Following a 30 second etch in the solution, the sample was rinsed in deionized water and ethyl alcohol. The etch was only moderately successful but more potent etches such as bromine in methanol also react with the aluminum film and the wires.

Elimination of etching through the use of planar techniques is the ultimate goal.

D. LEAD AND HOUSING ATTACHMENT

Aluminum wires were ultrasonically bonded to the aluminum film and to the Kovar extension on the housing using an ultrasonic bonder.

The TO-5 nickel cans were welded to the base by means of a capacity discharge welder.

VI. TESTING AND ANALYSIS

A. INCREASING AREA OF JUNCTION

Most work on gallium phosphide has been concerned with junction areas of the order of 1.6×10^{-3} cm^2. In the past, when the junction area has been increased by an order of magnitude to 1.6×10^{-2} cm^2, inconsistent results have been obtained in reverse breakdown voltage with respect to constant current density because of high dislocation density, poor structure and inhomogencity. A number of tests, therefore, were made on our material using both the smaller and larger area. It was found that the maximum reverse voltage breakdown attainable for the sample remained the same, even with an order of magnitude increase in junction area.

B. THERMAL CHARACTERISTICS OF ASSEMBLED RECTIFIERS

The temperature rise above ambient of a number of assembled rectifiers was measured to insure that the design of the structure and housing used was feasible. A thermocouple of chromel-alumel was welded directly to the housing to record the diode case temperature with the rectifier under full and continuous load (0.5 amperes D. C. forward current). The ambient temperature of the oven in which the diode was placed was recorded (see following paragraph VI (C) for further description). No unit was observed to fail because of mechanical failure (i.e. GaP chip detaching from base due to overheating or alloy material melting, etc.).

As expected, the units which had the lowest forward voltage drop (I_f = 0.5 amp) had the lowest diode case temperature. As a result of our tests, it was found that a temperature rise of 100 degrees above ambient (400°C) could be tolerated.

A list of some of the units tested and the temperature rise above ambient (for ambient temperature of 22°C and 400°C) is given in Table IV. A D. C. full load of 0.5 amperes was continuously applied to the rectifiers. The temperatures recorded are for steady state values of the rectifier characteristics. The rectifiers were unmounted, aside from attachment of leads for electrical contacts, and were operated in the free space environment of the oven. The differences noted in Table IV for the temperature rise above ambient may reflect differences other than the power loss generated in the forward direction. Such factors as position of the diode in the oven, the size of the lead wire for electrical contact, cooling by convection, radiation, proficiency of thermocouple contact to case, etc., may enter into the values noted. The values are important only as they infer a general

Table IV

TEMPERATURE RISE OF GaP RECTIFIERS
AT 22°C AND 400°C AMBIENT WITH ELECTRICAL CHARACTERISTICS

Sample	Ambient Temperature 22°C			Ambient Temperature 400°C		
	V (volts) Reverse at .1ma leakage	V (volts) Forward at 0.5 amp.	ΔT 22°C[1]	V (volts) Reverse at 5ma leakage	V (volts) Forward at 0.5 amp.	ΔT 400°C[2]
1R69G20-39	23.0	4.4	76	58.0	7.3	137
1R71G20-41	19.0	4.1	130	36.0	4.4	79
1R69G20-38	8.6	3.2	67	14.0	3.0	47
1R71G20-42	22.0	4.4	111	50.0	5.8	90
1NA73GP1-1-2	9.5	3.5	81	20.0	5.1	50
1R69-2-358-3 (100)	7.8	4.0	87	4.4	60.0	65
1NA74-029	10.6	2.1	41	13.5	1.8	21
1NA75-029	11.8	3.9	73	15.4	4.4	49

[1] Rise of diode case temperature above 22°C ambient.

[2] Rise of diode case termperature above 400°C ambient.

idea about diode case temperatures and estimates of junction temperature. (Junction temperatures may be between 10 and 50 degrees higher depending on the unit). An idea of the diode case temperature of two sample units for various ambient temperatures is provided in Figure 6. The two units chosen were 1NA74029 which had the lowest forward drop and 1R71G20-41 which appeared to have the highest diode case temperature at room temperature ambient. Rectifier 1NA74029 had an approximate continuous D. C. power dissipation of about 1 watt; whereas, 1R71G20-41 had a dissipation of about 2 watts. Measurements with both increasing and decreasing ambient temperature were made with good reproducibility as noted in Figure 6.

C. CURRENT-VOLTAGE CHARACTERISTICS, FORWARD AND REVERSE, AS A FUNCTION OF TEMPERATURE

A series of current-voltage measurements as a function of temperature have been made on rectifiers fabricated by the methods discussed in Section V. The units were attached to posts on a ceramic block. The posts were connected to external power sources for the forward and reverse measurements. Suitable metering was used to record the D. C. forward and reverse currents and voltages. Temperatures were measured with chromel-alumel thermocouples, one being attached to the housing and another used to measure ambient temperature. The thermocouple voltages were read on a thermocouple potentiometer.

The ceramic block containing the rectifiers was placed in a temperature controlled oven capable of attaining temperatures of 1000°C. Measurements of current, voltage and temperatures in general were made from room temperature to 400°C during both heating and cooling legs of a complete temperature cycle. In many cases the full load was applied continuously to the rectifier even when measurements were not being made. All of the units tested had junction areas of 1.6×10^{-2} cm^2.

A summary of the electrical characteristics is shown in Table V. Included in the Table are the carrier concentrations of the n type base material, the D. C. forward voltages at 0.5 ampere at both room temperature and at 5 ma at 400°C. ambient. The rectifiers are listed without regard to the junction technique used. From the table it is noted that unit 1NA79G20-41 had the best overall characteristics in that it had a D. C. reverse voltage of 180 volts at room temperature for a reverse current of 0.1 ma and a reverse voltage of 175 volts at 0.2 ma reverse current at 300°C. The forward drop at 0.5 amperes increased from 4.6 volts at room temperature to 5.7 volts at 300°C which was somewhat higher than desired but considerably better overall than found for many of the other samples. The unit was inadvertently destroyed by applying a large overvoltage during the testing at 300°C so that the characteristics at 400°C could not be measured.

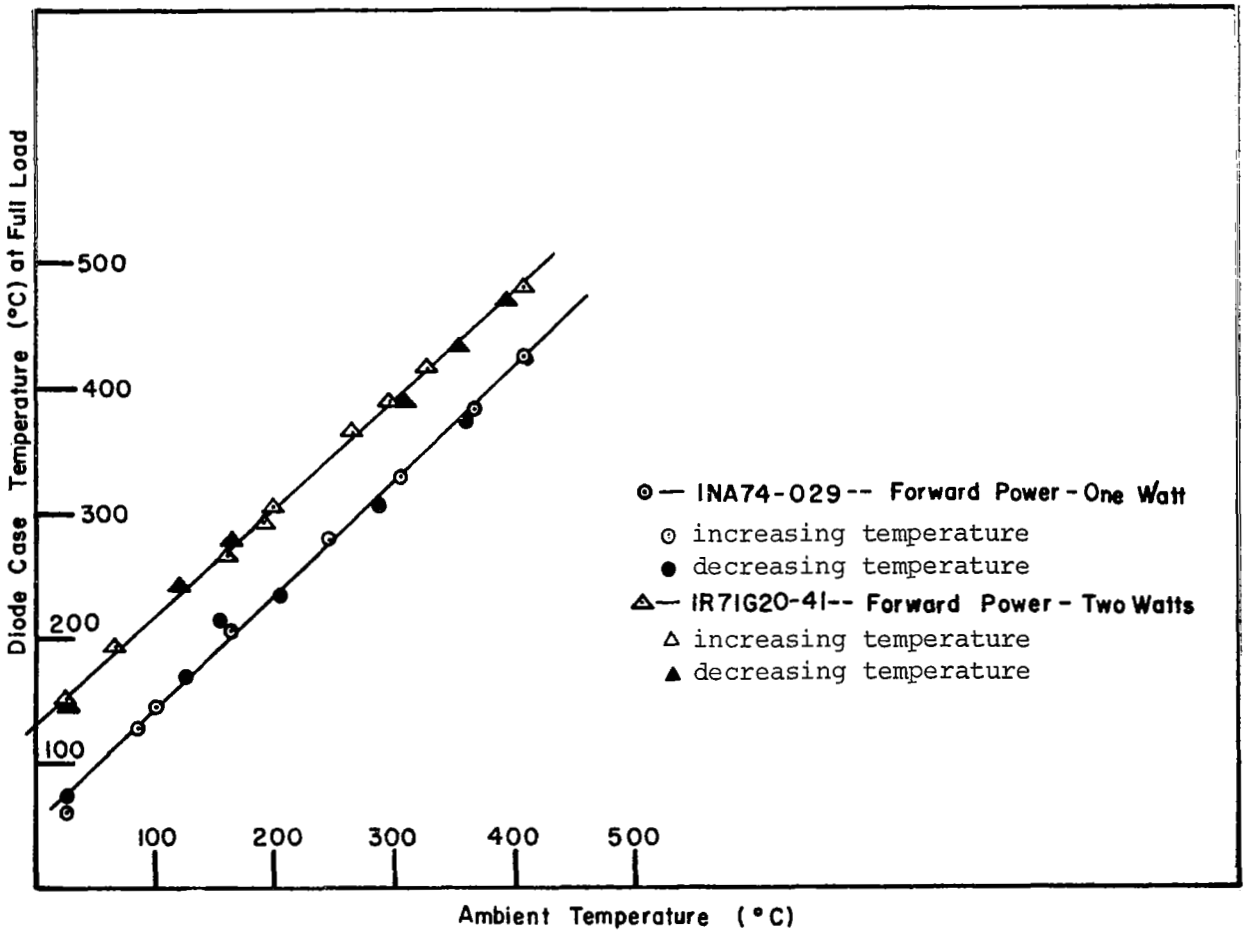

FIGURE 6. RECTIFIER CASE TEMPERATURE vs AMBIENT TEMPERATURE

Table V

SUMMARY OF ELECTRICAL CHARACTERISTICS OF RECTIFIERS TESTED

Sample	Carrier Concentration n_e of base material (no/cm^3), R.T.	D.C. V (volts) Reverse at .1ma (R.T.)	D.C. V (volts) Reverse at 5ma (400°C)	D.C. V (volts) Forward at 0.5 Amp (R.T.)	D.C. V (volts) Forward at 0.5 Amp (400°C)
2NA77G20-41	6.8×10^{16}	40.0	54.0	3.00	3.18
1R69G20-38	2.5×10^{17}	8.6	14.0	3.20	3.00
1NA74-029	2.5×10^{17}	10.6	13.5	2.10	1.75
1NA73GP1-1-2	2.6×10^{17}	9.5	20.0	3.50	5.08
1R69G20-39	6.4×10^{16}	23.0	58.0	4.40	7.30
1R69-2-358-3 (100)	4.3×10^{16}	7.8	60.5	4.07	4.40
1R71G20-42	5.6×10^{16}	22.0	50.0	4.40	5.80
1R71G20-41	6.8×10^{16}	19.0	36.0	4.10	4.40
1NA75-029	2.5×10^{17}	11.8	15.4	3.86	4.40
2NA76G20-39	6.4×10^{16}	70.0	112.0	7.90	20.20
1NA77G20-42	5.6×10^{16}	38.0	56.0	3.40	4.50
1NA76G20-40	3.6×10^{16}	52.0	75.0	4.60	8.60
1NA77MR # 1	8.6×10^{15}	20.0	37.0	11.10	12.60
1NA76G20-38	2.5×10^{17}	12.0	36.0	2.50	2.03
2R56G17-9	3.5×10^{16}	54.0	86.0	7.50	24.50
1R62PE051	3×10^{15}	24.0	45.0	15.50	15.30
1NA78GP1-4-1	3.6×10^{17}	19.0	33.0	2.58	1.98
2NA79G20-41	6.8×10^{16}	48.0	78.0	6.20	7.60
1NA79G20-41	6.8×10^{16}	181.0	175.0 [1]	4.60	5.70 [1]
1NA81G20-42	5.6×10^{16}	41.0	59.0	3.66	5.00
1NA80G20-39	3.6×10^{16}	48.0	86.0	4.30	12.90
1NA82G20-12-1	2.6×10^{16}	22.0	32.0	44.50 [2]	33.00 [2]
1NA79MR # 1	8.6×10^{15}	493.0	318.0 [3]	215.00 [3]	212.00 [3]
1NA81-MR-029	2.5×10^{17}	19.0	35.0	19.50	12.10
1NA79G20-39	6.4×10^{16}	38.0	52.0	9.60	7.50
Grown Jct # 1	$P_h = 9 \times 10^{17}$				
	$n_e = 1 \times 10^{17}$	17.0	-	20.00 [4]	-
Grown Jct # 2	"	22.0	-	18.00 [4]	-
Grown Jct # 3	"	20.0	-	21.00 [4]	-
Grown Jct # 4	"	16.0	-	6.00 [4]	-
Grown Jct # 6	"	17.0	-	7.20 [4]	-
Grown Jct # 8	"	17.0	-	5.80 [4]	-
3NA87G21-29-2	5×10^{16}	86.0	-	9.10	-
1NA87G21-29-2	5×10^{16}	102.0	-	9.00	-
2NA87G21-30-3	1.67×10^{16}	233.0	-	37.90	-
7NA87G21-29-2	5×10^{16}	90.0	-	8.10	-
4NA87G21-30-3	1.67×10^{16}	251.0	-	48.00	-

[1] taken at 300 °C Ambient

[2] taken with forward current of 0.2 amp rather than 0.5 amp.

[3] taken only to 200°C, forward currents were $\leq$ 1ma.

[4] forward voltage for forward current of 0.1 amp.

The lowest forward voltage noted at 400°C was for sample 1NA74029 with a value of 1.75 volts for 0.5 amperes. This was found for n type material of carrier concentration greater than $10^{17}/cm^3$. The highest D. C. reverse voltage found at 400°C for 5 ma leakage was with rectifier 2NA76G20-39 where a value of 112 volts was found. In each of the latter two units the other characteristic, i.e. either reverse characteristic or forward characteristic, was poor. The best overall unit with which we achieved 400°C, and which was reproducible, was 2NA77G20-41 where both the forward and reverse characteristics were fairly constant through the temperature range to 400°C and had a reasonable degree of reversibility.

Material G20-41 was of particular interest because it contained two donor impurities, sulfur and tellurium, with tellurium being present in an amount about double the sulfur. A study was made of this material as a function of the various junction techniques used and compared with other materials. This will be reported below.

1. Forward Voltage Characterisitcs with Temperature

The effect of D. C. forward voltage drop as a function of ambient temperature for various forward currents is shown in Figures 7, 8, and 9. In some of the cases we have also shown the cycling of the I_f-V_f characteristics with temperature. Three forward currents (100 ma, 300 ma, 500 ma) were plotted for each of the samples used for the figures. At 100 ma, the forward voltage decreases with increasing temperature as one would expect from theory. At the higher currents, the forward voltage did not behave as predictably, indicating the likelihood of influence by deep levels. Whether the voltage drop increases or decreases appears to be related to the extent of the deep levels present in the starting material. The processing method may influence the extent of the change in the forward drop but not the general characteristic. A good example of this is illustrated in Figure 7 for material G20-41. Junctions were diffused into the material at 800°C (1R71G20-41) 875°C (2NA77G20-41) and by the solid-solid diffusion technique (1NA79G20-41, 2NA79G20-41). It can be seen that in spite of differences in the magnitude of the forward voltage drops for the various diffusion techniques, the general shape of the characteristic for the three currents was similar. Where the sample has been cycled, a "hysteresis" effect was present for all the runs. Generally at 0.5 amp, the forward voltage drop increased with increasing temperature. At 100 ma forward current, the forward voltage decreased with increasing temperature whereas at 300 ma, the behavior of forward voltage with temperature reflected a characteristic between the above two cases. Generally for our "junction" type (whether P-I-N, M-I-N, M-N, etc.) structure we had to consider both the effect of injection into a high resistivity layer (i layer) and the variation of the resistivity of the i layer with temperature (and as a consequence the position of the Fermi level in the i layer).

Use was made of the level of the zinc concentration and gradient to note the presence of deep levels. Because the lifetimes may be short

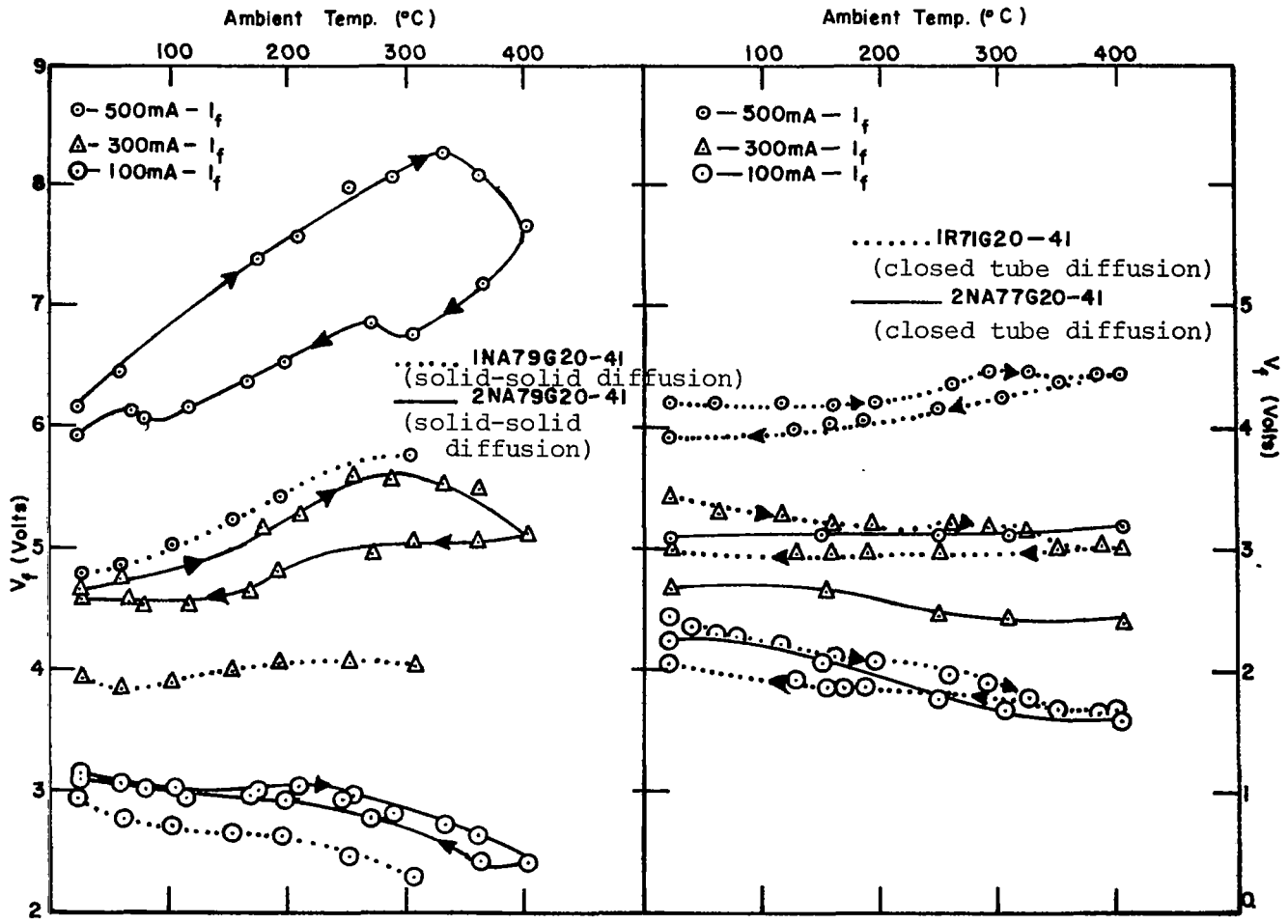

FIGURE 7. FORWARD VOLTAGE DROP AS A FUNCTION OF TEMPERATURE FOR VARIOUS FORWARD CURRENTS

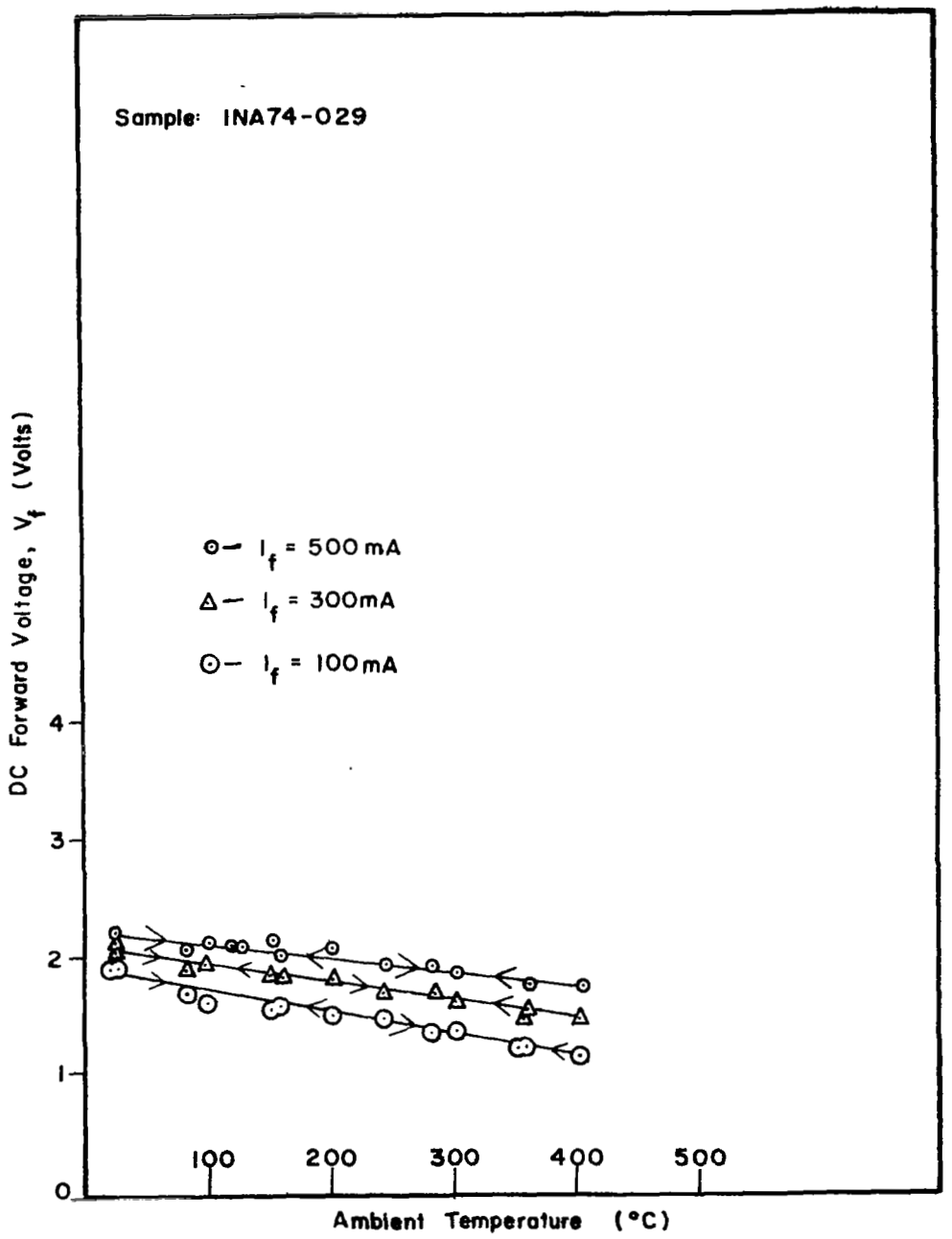

FIGURE 8. FORWARD VOLTAGE DROP AS A FUNCTION OF TEMPERATURE FOR VARIOUS FORWARD CURRENTS

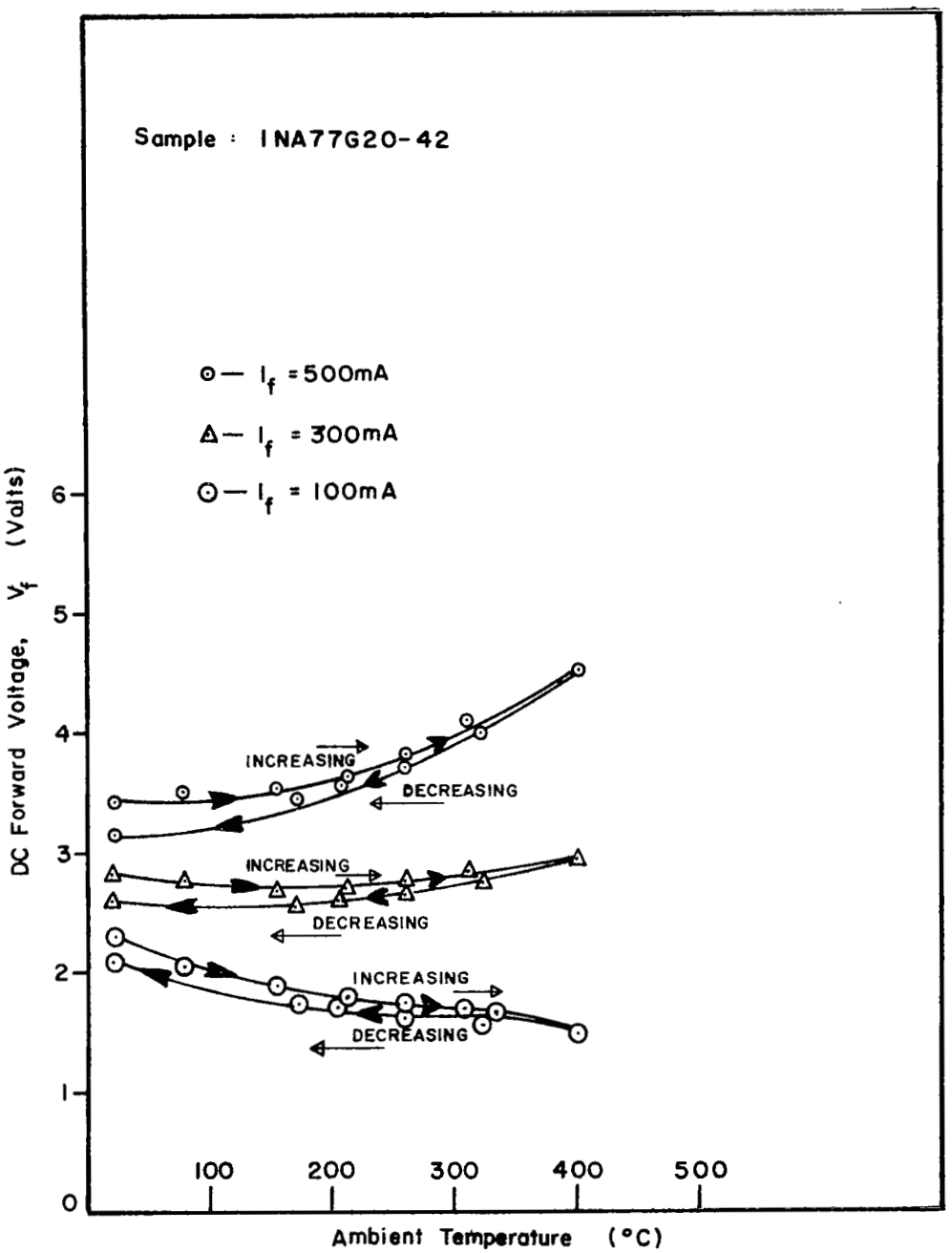

FIGURE 9. FORWARD VOLTAGE DROP AS A FUNCTION OF TEMPERATURE FOR VARIOUS FORWARD CURRENTS

($\sim 10^{-8}$ to 10^{-9} sec), leading to short diffusion lengths, the high resistivity layers formed in the junction fabrication may be too wide to effectively provide for low voltage drops. Essentially, minority carrier injection was small for carrier concentrations below $10^{17}/cm^3$. Above this value of concentration the effects of deep levels and background can be overcome by the larger effect of the free carrier concentration. Injection becomes considerably better and the forward voltage drop behaves as expected from theory, namely decreasing voltage with increasing temperature. This is shown in Figure 8 for sample 1NA74-029. At the same time, there is little or no "hysteresis" effect on heating and cooling the rectifier. We note that from a room temperature value of about 2.2 volts at 0.5 amperes, the forward drop decreased to 1.75 volts at 400°C ambient. The problem of high forward voltage then appeared to be associated with deep level impurities, vacancies, etc., which become important for carrier concentrations in the range below $10^{17}/cm^3$. However, to obtain high reverse voltages, it was necessary to work at the low 10^{15} to $10^{16}/cm^3$ carrier levels.

To more closely scrutinize the possible impurities which can contribute to the deep levels or to the high resistivity layer formed in junction diffusion, it is well to look at sample 1NA77G20-42 (diffusion at 875°C) and the impurity analysis of G20-42 as given in Table II. The forward characteristics are shown in Figure 9. The effect of temperature on forward voltage drop for this diffusion was more pronounced than for the same diffusion for G20-41 (Figure 7, 2NA77G20-41). From mass spectrometer analysis of these samples (Table II) we noted that the most pronounced differences in impurities were with nitrogen and tellurium. The effect of nitrogen, an isoelectronic substituent, on the rectifier characteristic is not clear, but tellurium does have a role as a group VI donor. While the additional appearance of the tellurium would suggest that the room temperature carrier concentration of G20-41 should be at least a factor of 3 greater, surprisingly it was found that G20-41 and G20-42 have about the same R. T. carrier concentration. It is suggested that tellurium may be playing an additional role to that of a substituent shallow donor, perhaps in complexing or inactivating some of the deep levels.

Perhaps an equally interesting comparison can be made with material G20-39. Rectifier 2NA76G20-39 formed by diffusion of zinc at 875°C from a closed tube shows considerably higher forward voltage drop (see Figure 10 for forward drop vs. temperature curve) than either rectifiers made from G20-41 or G20-42. Since the thickness of the gallium phosphide and the junction area were the same as for the other units and the carrier concentration was about the same as for G20-41 and G20-42 (Table I), the major voltage drop was in the high resistivity "i" layer. From Table II we noted that the major differences between G20-39, and G20-41 and G20-42 was in the amounts of nitrogen and, in the fact, that G20-39 contains no additional donor such as tellurium. From our discussion above, we would suggest that the absence of tellurium might account for the greater forward drop noted in unit 2NA76G20-39. If this

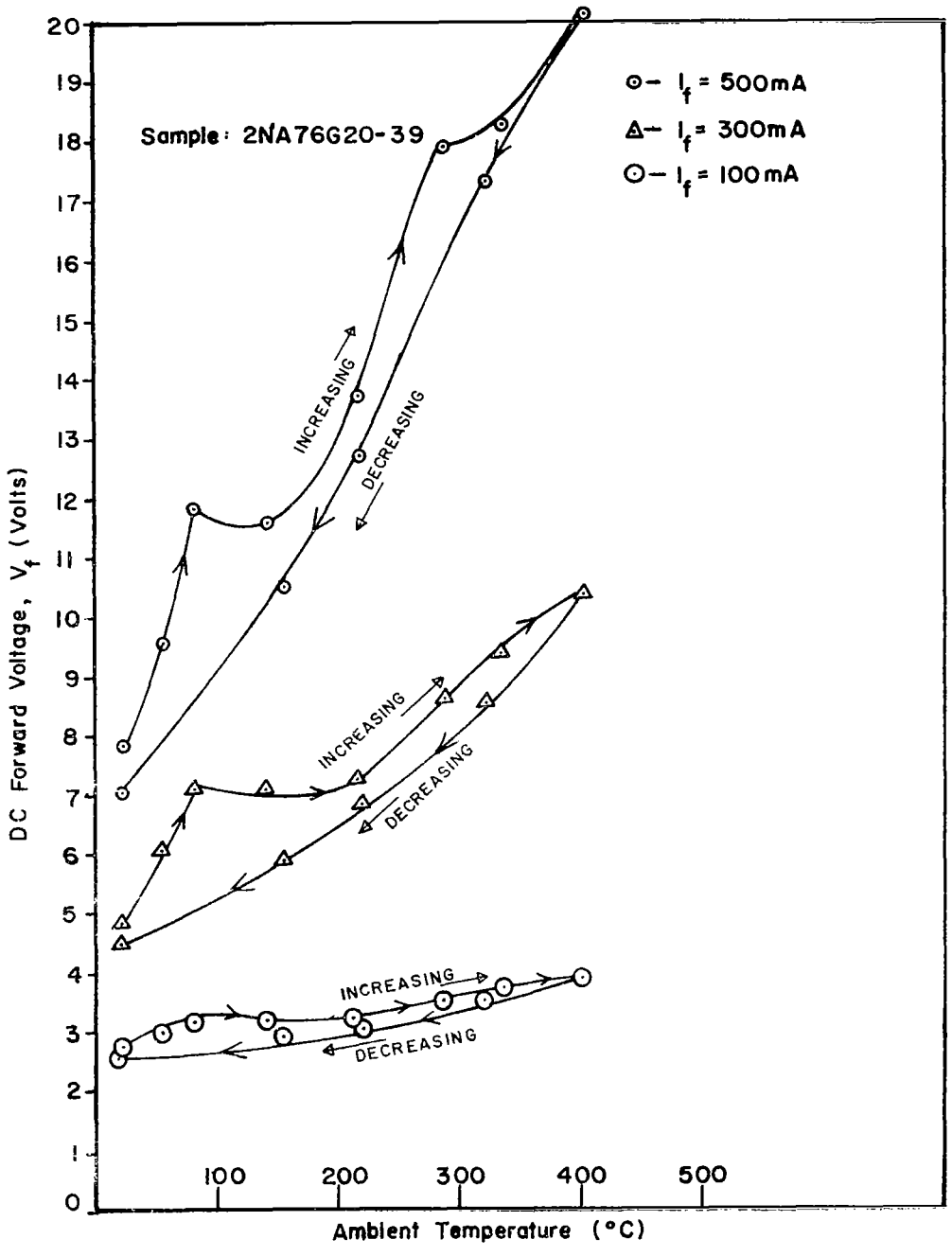

FIGURE 10. FORWARD VOLTAGE DROP AS A FUNCTION OF TEMPERATURE FOR VARIOUS FORWARD CURRENTS

is indeed the situation, then one might suggest the introduction of additional shallow level impurities (or even isoelectronic impurities) to electrically inactivate some of the deep levels.

An interesting empirical relationship originating as an outgrowth of the above discussion has been the grouping of impurities as deduced from the mass spectrometer analysis into a single factor and to relate this derived factor to the forward voltage drop at 0.5 amperes forward current (at room temperature). A factor so devised is the following: $[C/O/N_D]/n_e$ where C is the concentration of carbon atoms found from mass spectrometer analysis, O is the oxygen concentration similarly determined. $N_D = \Sigma$ (S + Si + Te + Se + Sn + ---); n_e is the total electrical carrier concentration of the base material at room temperature. Figure 11 is a plot of the forward voltage drop at R. T. (1/2 ampere forward current, same junction area) for samples having various $[C/O/N_D]/n_e$ factors and for two zinc diffusion temperatures. The significance of the factor is that it should be as small as possible. This can be accomplished in several ways: one is to make the carrier concentration large. Unfortunately, this leads to low breakdown voltages. If, however, we take a value of 0.25 for the factor $[C/O/N_D]/n_e$ and set $n_e = 1 \times 10^{16}/cm^3$, and adding 5×10^{16} atoms/cm^3 of S and Te doping while keeping the oxygen level to $2.5 \times 10^{16}/cm^3$, the condition for obtaining low forward voltage drops of 3 volts then is to keep the carbon level below $10^{16}/cm^3$. At the same time the low carrier level should meet the requirement for obtaining reverse breakdown voltages of 100-150 volts. There is a hint that the C/O (carbon/oxygen) ratio is tied in with defects and impurity complexes.

We have attempted to look at the high resistivity "i" layer from another point of view: namely, double injection or space charge limited current theory. We chose rectifiers made from GaP material G20-41 and selected samples which had been zinc diffused via closed tube diffusion at 875°C and 800°C and via solid-solid diffusion. Subtracting the junction or barrier voltage from the forward drop a current-voltage plot on a log-log scale of the high resistivity region (at room temperature) of the samples diffused via the closed tube process shows a current-voltage variation of I-V whereas for the solid-solid diffusion, one finds a $I\text{-}V^{1.3}$ relationship. The meaning of the difference is not understood.

2. Reverse Voltage Characteristics with Temperature

The reverse voltage is basically determined by the impurity doping level of the more lightly doped region in a p-n junction. If, as is usually the case, the base n layer is the lighter doped, then the maximum obtainable breakdown voltage will be given by the base carrier concentration (see Figure 1). The breakdown voltage should increase with increasing temperature according to the work of McKay[9] and Crowell and Sze[10] and Sze[11]. A simple explanation for this increase is that the hot carriers passing through the depletion layer under high field lose part of their energy to optical phonons

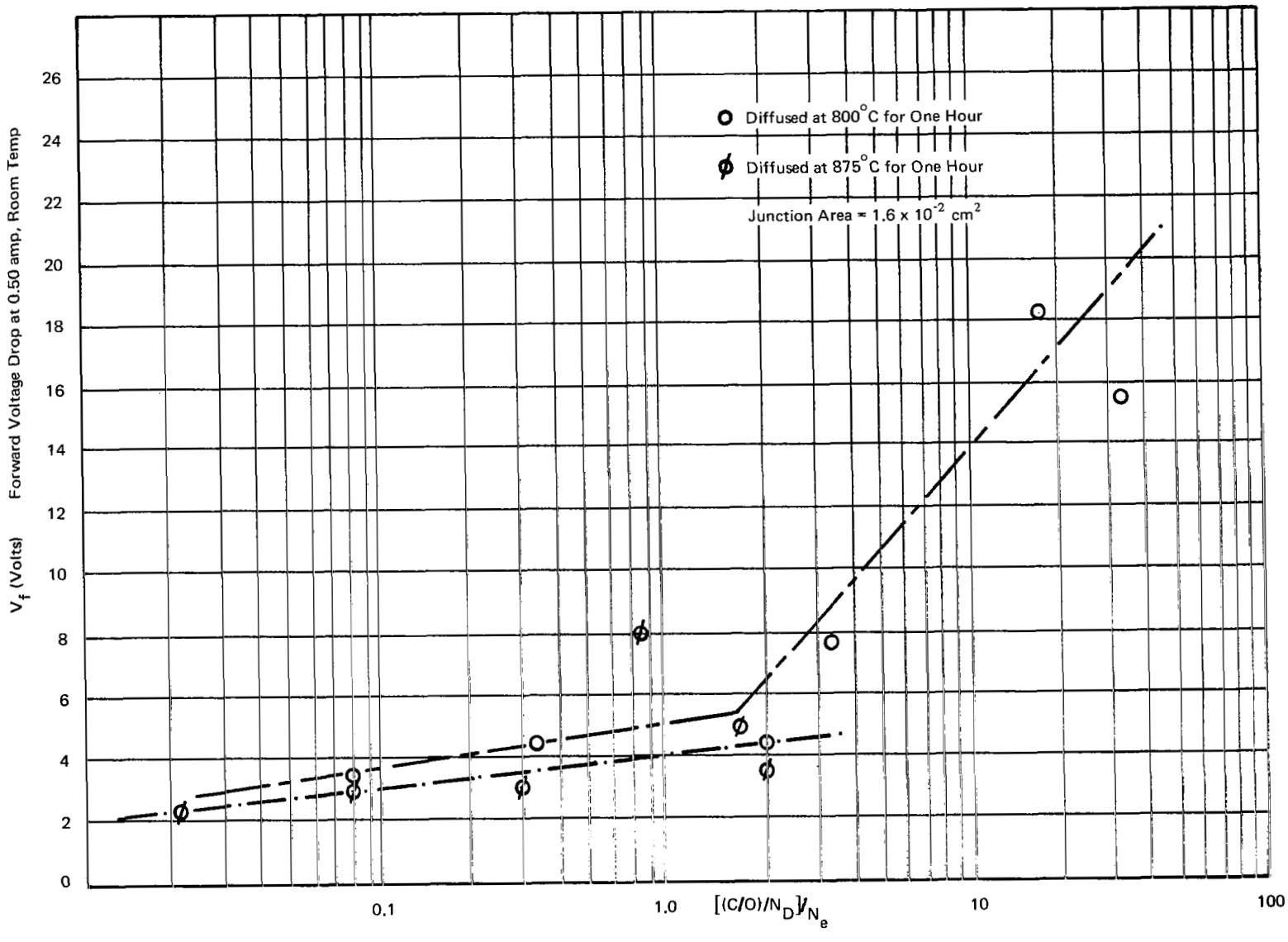

FIGURE 11. FORWARD VOLTAGE DROP vs $[(C/O)/N_D]/N_e$
(See Text for Meaning of Symbols)

after traveling each electron-phonon mean free path, λ . The value of λ decreases with increasing temperature. Therefore, the carriers lose more energy to the crystal lattice along a given distance at constant field. Hence, the carriers must pass through a greater potential difference (or higher voltage) before they can acquire sufficient energy to generate an electron-hole pair. Sze[11] indicates that for the same doping profile the predicted percentage change on the breakdown voltage with temperature is about the same for GaP as it is for Si junctions. The variation of voltage breakdown with temperature can be expressed as[9]

$$V_B(t) = V_B(t_o)\ [1 + \beta'(t-t_o)] \quad - - - - - - - - - - - - - - - (1)$$

where $V_B(t_o)$ and $V_B(t)$ are the breakdown voltages at temperatures t_o (room temperature) and t respectively, β' is the temperature coefficient of the breakdown voltage.

From the curves of Crowell and Sze[10] the ratio of $V_B(t)/V_B(t_o)$ should increase 20 to 40% at 400°C depending on the background doping levels.

We have plotted the D. C. reverse voltage for various rectifiers fabricated from material G20-41 using different junction processing techniques. According to Figure 1, G20-41 with a room temperature background doping concentration of 6.8×10^{16} should have a theoretical voltage breakdown at room temperature of approximately 40 volts and at 400°C the breakdown should be about 55 volts. In Figure 12, a, b, c, the D. C. reverse voltage of samples IR71G20-41, 2NA77G20-41, 1NA79G20-41 and 2NA79G20-41 are plotted as a function of temperature. The first two samples have been zinc diffused at 800°C and 875°C respectively in a closed tube, the latter two samples were fabricated by the solid-solid diffusion technique. Sample 1NA79G20-41 was inadvertently broken down at 300°C when a large over voltage was applied and consequently the data only goes to 300°C.

The D. C. reverse voltages obtained in Figure 12 for material G20-41 by the different processing techniques indicate a range of values (at 100 μa leakage) between 18 volts and 180 volts. Two of the samples fall within the voltage breakdown predicted by Figure 1. It is interesting to note that the D. C. reverse voltages obtained with G20-41 by the solid-solid diffusion are higher than noted with the closed tube diffusion and higher than expected from simple p-n junction theory of breakdown. This suggests that perhaps there is an additional barrier or the lightest doped side is not the base n layer. The solid-solid technique was generally found to give higher D. C. reverse voltages than found by other techniques (see Table VI).

With permitted leakage values of 5 ma it can be seen from Figure 12 C that values as high as 200 volts may be expected. The reverse voltage at this leakage level increases with increasing temperature generally.

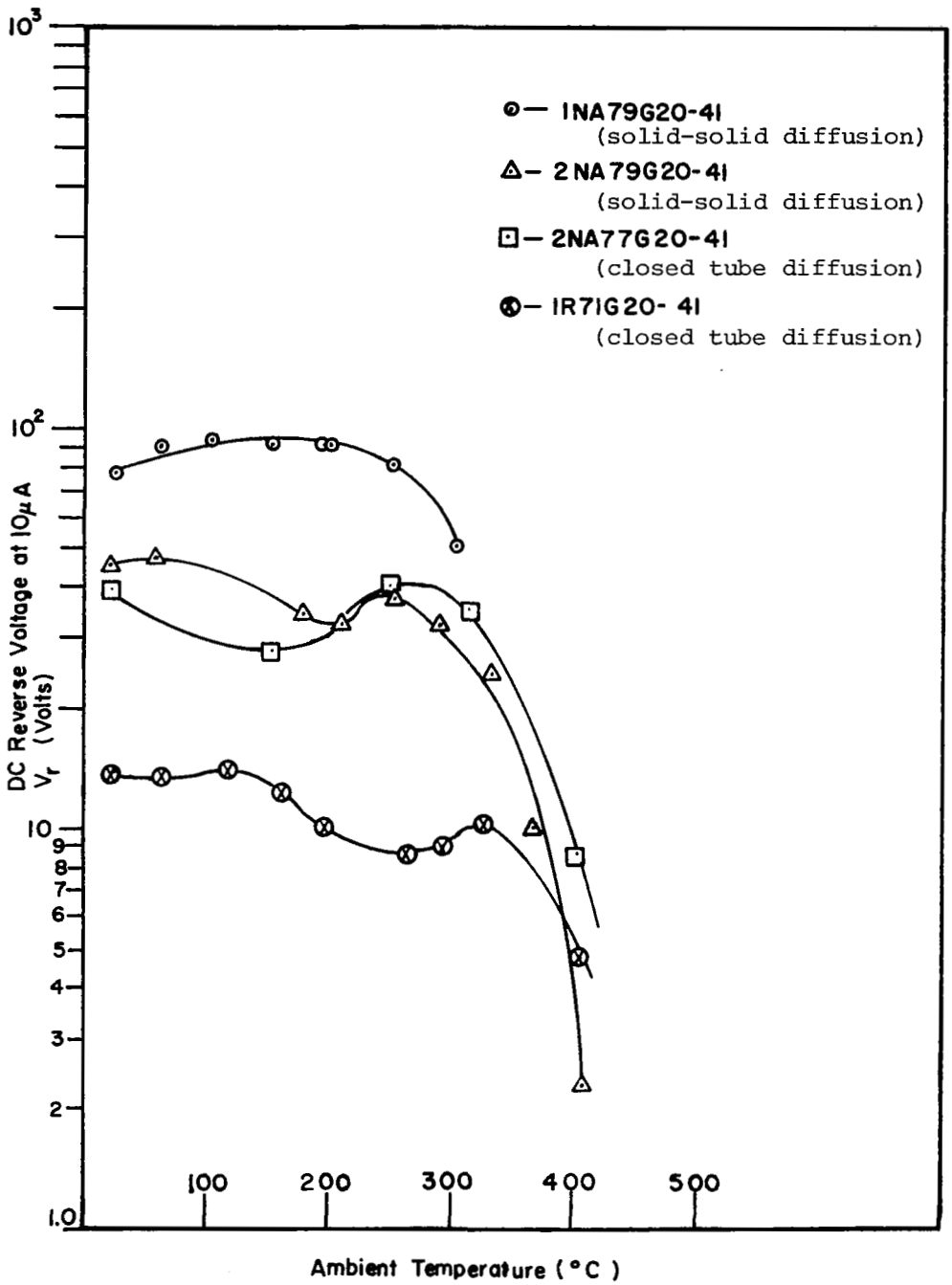

FIGURE 12(a). CYCLIC VARIATION OF D.C. REVERSE VOLTAGE (AT 10 a REVERSE CURRENT) WITH TEMPERATURE

(For Four Rectifiers Processed Differently From Material G20-41)

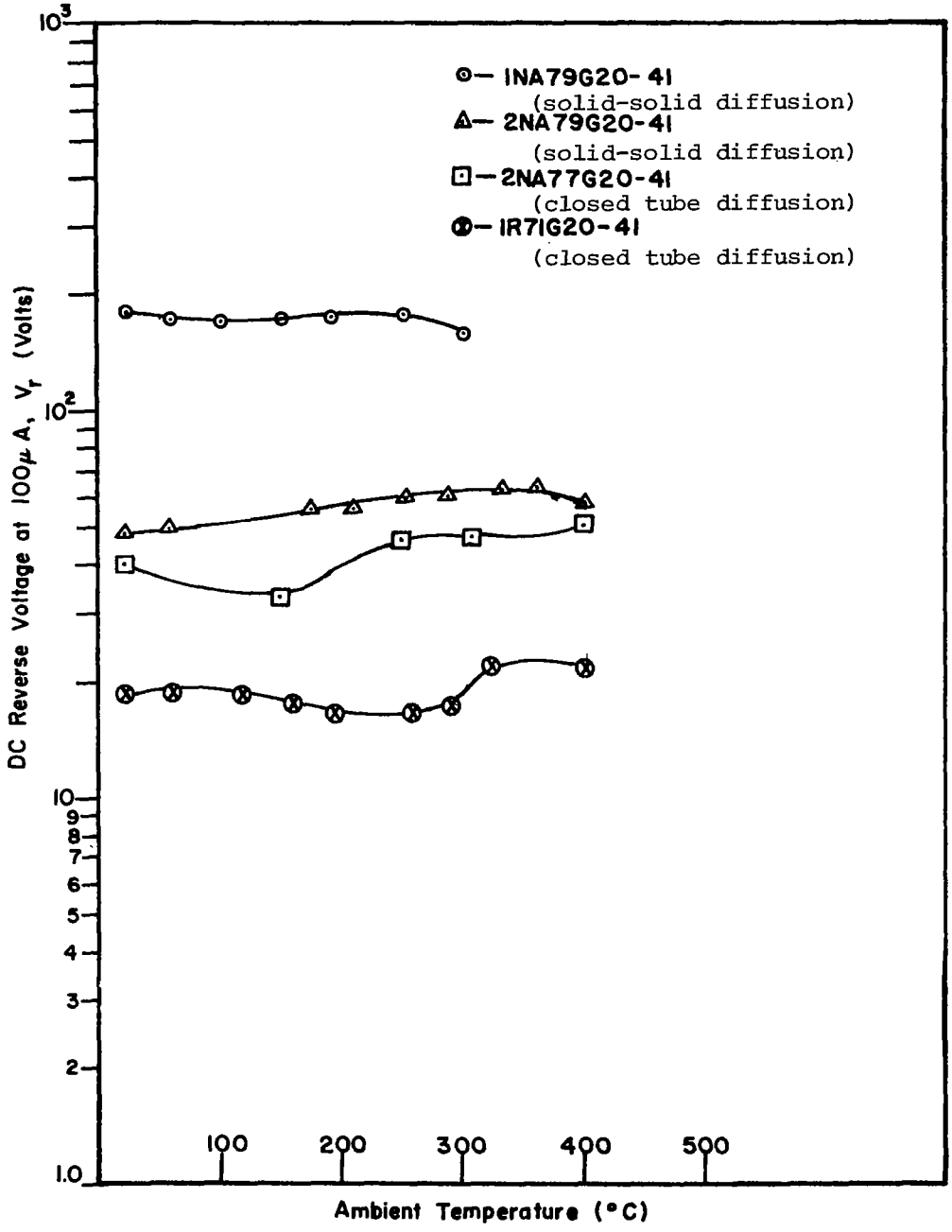

FIGURE 12(b). CYCLIC VARIATION OF D.C. REVERSE VOLTAGE (AT 100 μa REVERSE CURRENT) WITH TEMPERATURE

(For Four Rectifiers Processed Differently From Material G20-41)

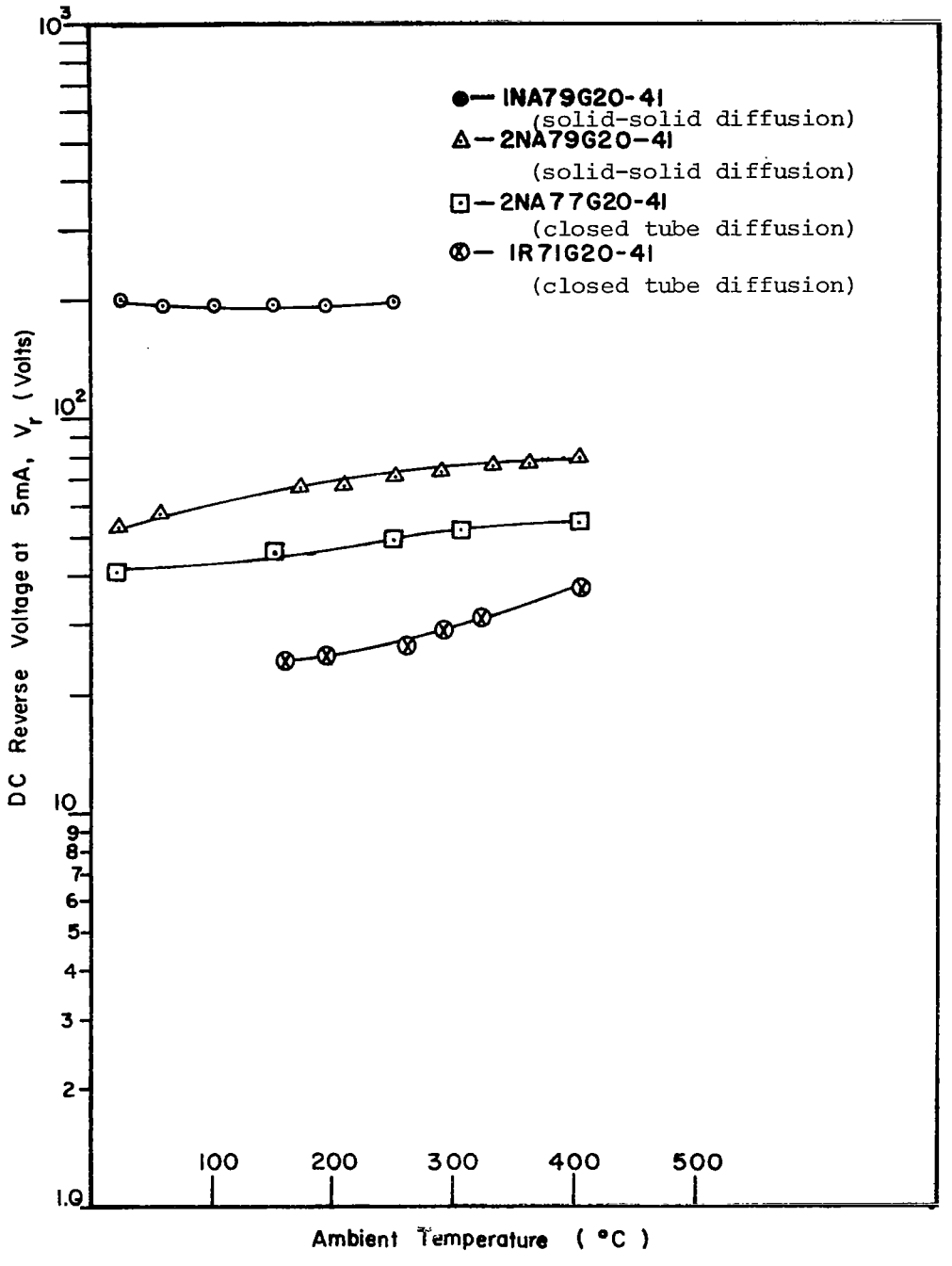

FIGURE 12(c). CYCLIC VARIATION OF D.C. REVERSE VOLTAGE (AT 5 ma REVERSE CURRENT) WITH TEMPERATURE

(For Four Rectifiers Processed Differently From Material G20-41)

Table VI

ELECTRICAL CHARACTERISTICS OF GaP PROCESSED BY SOLID-SOLID DIFFUSION TECHNIQUE

(a) Room Temperature

Sample[1]	D. C. Forward Characteristics V_f (volts) 100ma	300ma	500ma	D. C. Reverse Characteristics V_R (volts) 10μa	100μa
MR 1	215.0[2]	-	-	84	493
G 20-40	15.0	25.0	35.0	45	81
1NA79G20-41	2.8	3.8	4.6	95	180
2NA79G20-41	3.2	4.7	6.3	48	48
NA87G21-29-2	3.4	5.4	7.0	95	115
NA87G21-29-2	5.0	7.0	8.5	65	70
NA87G21-30-3	5.0	9.0	12.0	40	50
NA87G21-30-3	5.0	11.0	17.0	170	210

[1] Junction areas of the samples are all the same (i.e. 1.6×10^{-2} cm ^{2}).

[2] At current of .01 ma.

Table VI (cont'd)

ELECTRICAL CHARACTERISTICS OF GaP PROCESSED BY SOLID-SOLID DIFFUSION TECHNIQUE

(b) 400°C Ambient

Sample	D. C. Forward Characteristics V_f (volts) 100ma	300ma	500ma	D.C. Reverse Characteristics V_R (volts) 100μa	5μa
1NA79G20-41	2.3	4.0	5.7	159[1]	175[1]
2NA79G20-41	2.4	5.1	7.6	55	78
G20-40	21.0	30.0	37.0	50	97

[1] Sample was inadvertently broken down at 300°C by applying a large over voltage. The reverse voltage measurement was that recorded at 300°C for a leakage of 200μa.

The high level of leakage can generally be tolerated when the total power dissipation in the reverse direction is less than 10% that in the forward direction. The variation of the reverse voltage with temperature noted for the four samples at a reverse current of 100 μa is given in Figure 12 B. The reverse voltage shows some change with temperature, but it is not appreciable. As expected, the most sensitive indication of changes is found in Figure 12 A where the D. C. reverse voltage is plotted as a function of temperature for the four samples at a reverse leakage of 10 μa. Two effects are noted in the figure: one is an initial decrease of V_R with increasing temperature to about 250°C; a second effect is noted above about 250°C and especially above 300°C where a more rapid decrease of reverse voltage with temperature is observed.

Several factors, aside from surface leakage, could be contributing to the decrease of reverse voltage with increasing temperature for a given reverse current. These are (1) deep level impurities (2) crystal strain and defects (poor crystal structure) (3) mobility of zinc interstitials.

As temperature increases, deep levels can become an additional source of carriers and deep level impurities such as oxygen or oxygen dominated complexes can play an important role in accounting for the leakage currents and, in effect, may raise the level of leakage current at a particular reverse voltage.

The effects of strain and dislocations introduced into the crystal during growth can result in the formation, during zinc diffusion*, of zinc aggregates, complexes, precipitates forming at these defect or dislocation sites.[12, 13, 14] As the temperature increases and a reverse or bias voltage is applied, zinc interstitials, which are not tightly bound, can become mobile leading to increased leakage as well as irreversible changes in the device characteristics.

The effect of deep levels should not result in a pronounced irreversibility whereas, the effect of zinc mobility (and poor structure) could result in a very pronounced degradation of characteristics on cycling. In Figure 13 we have plotted the results of cycling the reverse voltage (at 10μ a leakage) of two samples as a function of temperature in the range between room temperature and 400°C. One of the samples, 1R71G20-41, which was fabricated by zinc diffusion in a closed tube shows a large irreversibility in cooling from 400°C. The unit never returns to its original value. It is believed that the degradation arises through increased mobility of zinc atoms which can lead to junction shorting. This situation results from a combination

---

*especially when the zinc surface concentration is too high and not well controlled.

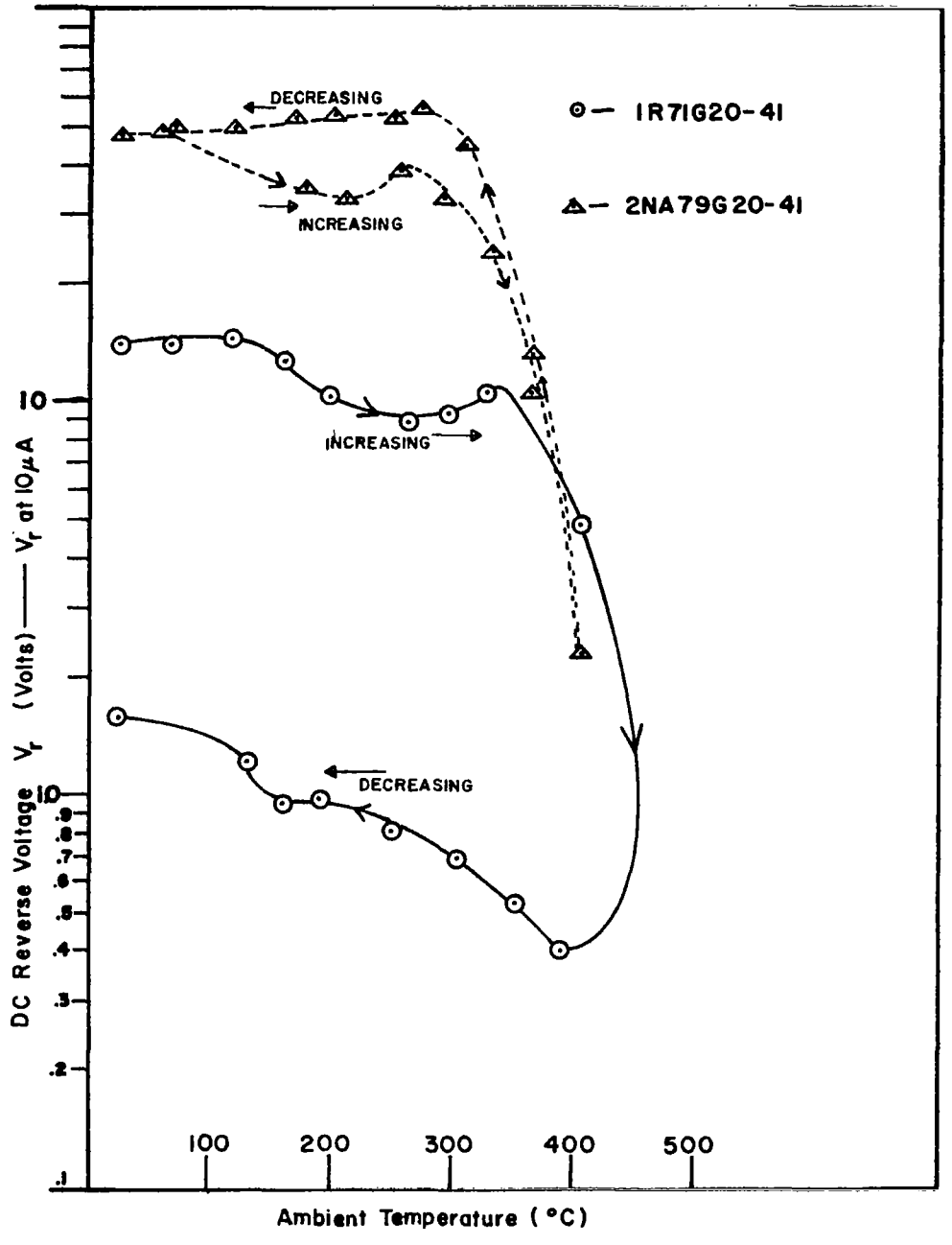

FIGURE 13. CYCLIC VARIATION OF REVERSE VOLTAGE AT 10 μa REVERSE CURRENT WITH TEMPERATURE (Samples IR71 G20-41 and 2 NA 79 G20-41)

of inadequate control of zinc surface concentration and poor crystal structure. The heavy concentration of zinc at the surface permits rapid diffusion of zinc interstitials and they tend to move more rapidly along faults, dislocations, etc., forming aggregates, precipitates and complexes with defects, deep level impurities, etc.

The result of better control of zinc is shown by the much more reversible result obtained in Figure 13 with sample 2NA79G20-41, fabricated by the solid-solid diffusion technique. The "hysteresis" effect in the temperature range of 200-300°C is believed due to deep level effects and perhaps insufficient time to establish equilibrium at these temperatures. The large drop in reverse voltage above 300°C may be related to the poor structure or high dislocation density of the material G20-41. The exact nature of the effect is not known.

The important factor is that close and careful control of zinc concentration can reduce degradation effects in the electrical properties of the rectifiers and also reduce but not eliminate the dependence of the voltage and current characteristics on the structure.

Sample 1R71G20-41 is fairly typical of results obtained where the zinc concentration was not controlled adequately for the poor crystal structure. (see Figure 13.)

To more clearly show the effect of structure, we compared sample 1R71G20-41 with 2NA76G20-39. Both samples were zinc diffused via the closed tube, but material G20-39 had a dislocation density of 8×10^5 etch pits/cm^2; whereas, G20-41 had a dislocation density of 3.5×10^6 etch pits/cm^2, a factor of over four higher. A plot of D. C. reverse voltage vs. temperature at a reverse leakage of 10 μa is given in Figure 14. The cycling of the units reveals a significant difference in reversibility, the sample with the better structure, lower dislocation density (2NA76G20-39), has the more reproducible characteristics.

Supportive evidence for improving the structure of the gallium phosphide grown, decreasing effect of deep level impurities such as oxygen, and very closely controlling the zinc concentration and diffusion appear from the current-voltage characteristics of the rectifiers as a function of temperature.

D. SOME ELECTRICAL CHARACTERISTICS OF SAMPLES PREPARED BY SOLID-SOLID (OXIDE) DIFFUSION TECHNIQUES

The solid-solid diffusion process discussed in Section V has produced some interesting current-voltage characteristics as well as the best overall I-V characteristics of those GaP rectifiers fabricated. Sample 1NA79G20-41 was prepared using the solid-solid diffusion process.

Current-voltage traces of rectifier 1NA79G20-41 room temperature characteristics are shown in Figure 15 a, b, c. In Figure 15 a, at about 2 ma forward current and 2.5 volts, a negative resistance effect is noted. As the current is increased to 0.5 amperes (Figure 15 b),

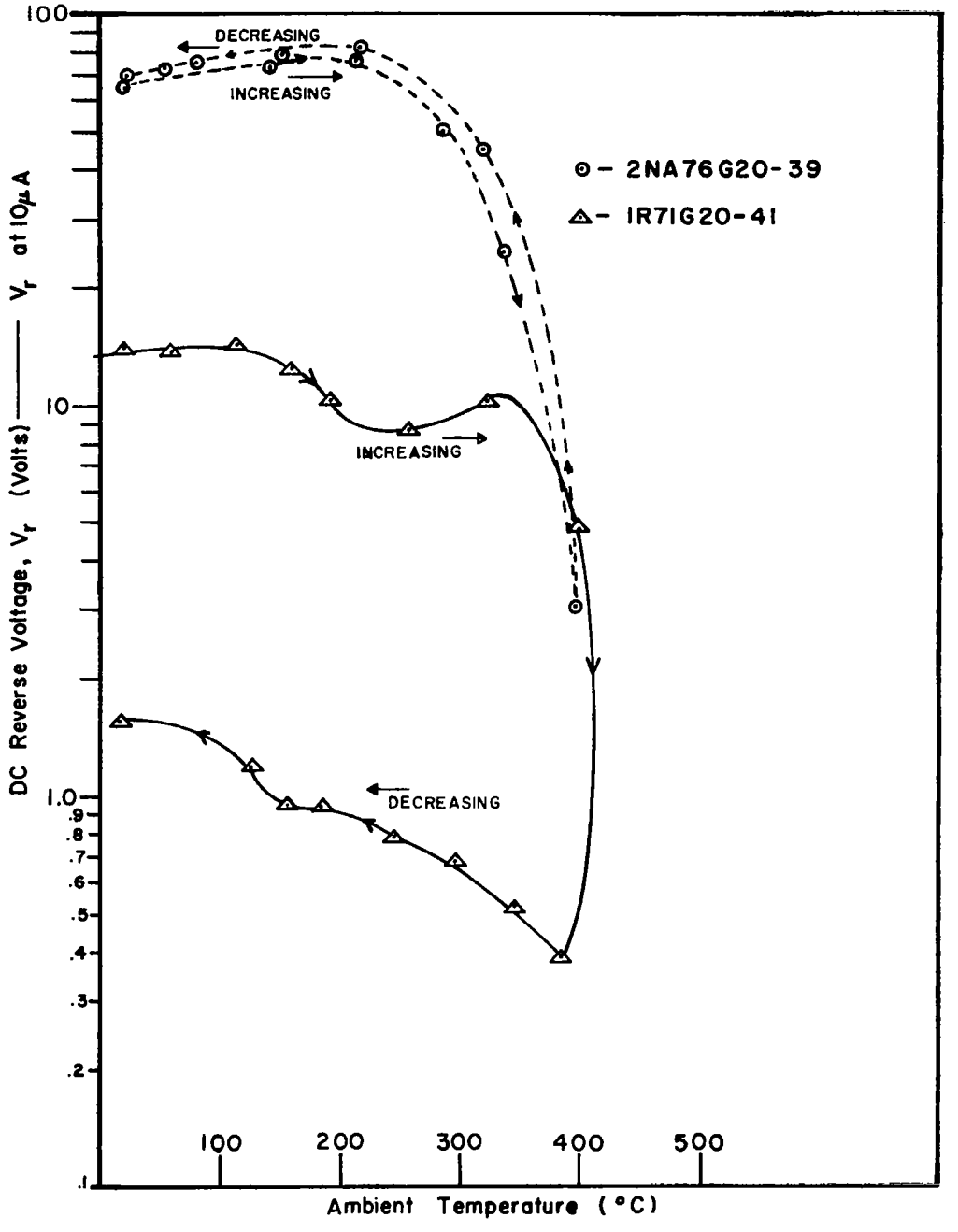

FIGURE 14. CYCLIC VARIATION OF REVERSE VOLTAGE AT 10μa REVERSE CURRENT WITH TEMPERATURE SHOWING DIFFERENCES IN RECTIFIERS – MADE FROM MATERIAL G20-41 AND G20-39. MATERIAL G20-39 HAS LOWER ETCH PIT DENSITY THAN G20-41

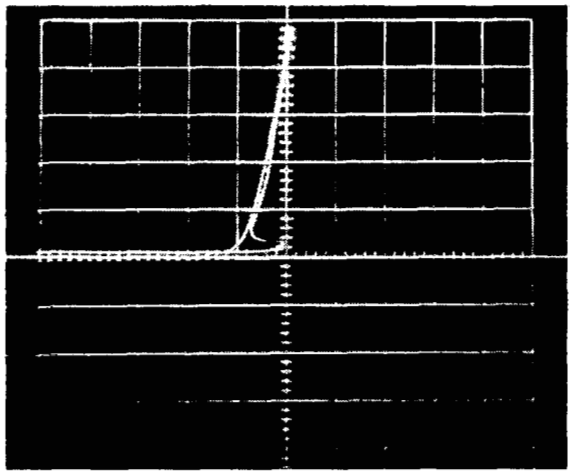

(a) Forward Characteristics at low currents showing negative resistance; horizontal scale, voltage, 5 volts/div., vertical, current 10 ma/div.

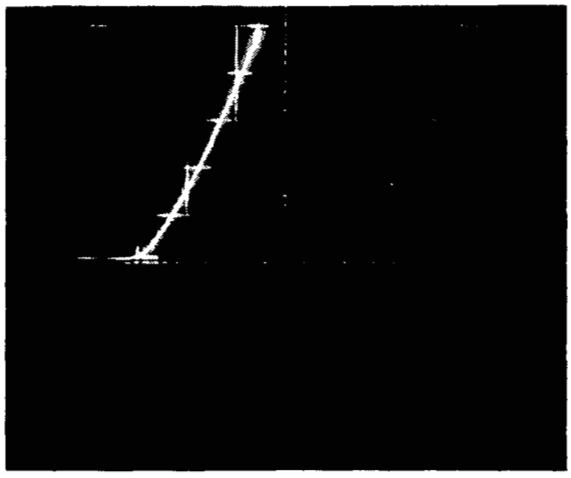

(b) Forward characteristics at high currents horizontal - 1 volt/div; vertical - 100 ma/div.

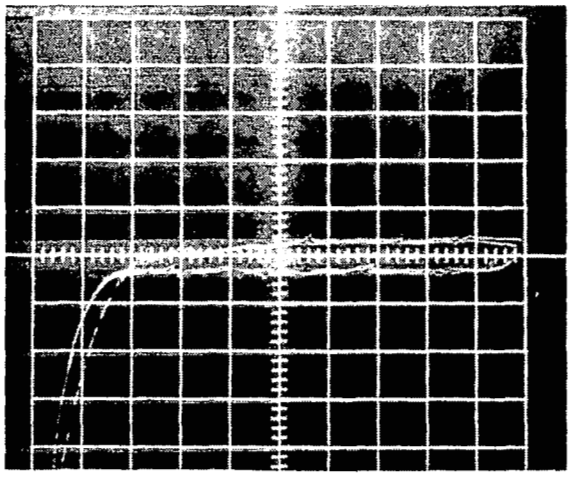

(c) Reverse characteristics - horizontal - 20 volts/div; vertical ma/div.

FIGURE 15. I-V OSCILLOSCOPE TRACES AT ROOM TEMPERATURE OF SAMPLE IN A 79 G20-41 USING SOLID-SOLID DIFFUSION PROCESS

the forward voltage increases to about 4.6 volts. While there is no straight forward injection, the presence of the negative resistance region does tend to reduce the value of forward voltage below that expected. The D. C. reverse voltage-current characteristic is shown in Figure 15 c (the reverse voltage scale is 20 volts/division). A breakdown is noted to occur at about 180 volts. The vertical scale is 10 μa/division.

Although the negative resistance effect noted in Figure 15 a has not been explained, it is speculated that it could be attributed to a double injection mechanism, internal field emission or a breakdown mechanism. While there is an absence of real injection after the negative resistance, the forward drop is lower at 0.5 amperes than would be the case without the negative resistance effect. The lack of a real injection effect points, as has been inferred previously, to the presence of deep levels and poor structure. These factors can lead to short diffusion lengths and low lifetimes. The situation is especially pronounced for carrier concentrations below $10^{17}/cm^3$.

Another effect noted with use of the solid-solid diffusion process is that shown in Figure 16. This is a room temperature forward current-voltage trace found in sample lNA84GP2-2-2 showing oscillations. The current level is about 0.4 ma where the effect is observed.

A list of current-voltage characteristics of samples processed by the solid-solid diffusion technique is given in Table VI.

As pointed out previously, the reverse voltages obtained are higher than found when processed by other techniques.

Some of the units listed in Table VI were not taken to 400°C because it was felt that the results would not provide any additional information.

E. CAPACITY-VOLTAGE MEASUREMENTS ON FABRICATED RECTIFIERS

Capacity-voltage measurements taken at 1 megacycle using capacitance bridge have suggested that the surface concentration of zinc appears to be greater for the closed tube zinc vapor diffused technique than by using the solid-solid diffusion process. Capacity measurements on units made by the former process are (for an area of 1.6×10^{-2} cm^2) of the order of 300-800 pf; whereas, for the same area, but using the solid diffusion process the highest capacities achieved are about 75 pf.

An outgrowth of these measurements has been the relationship between the forward voltage drop at 0.5 amperes (at room temperature) and the zero bias capacitance (for an area of 1.6×10^{-2} cm^2). It has been found that there is an inverse relationship between capacity and forward voltage as indicated in Figure 17. It is desirable using the solid-solid diffusion process to aim for zero bias capacities of about 350 pf which is a factor of 5 higher than presently achieved.

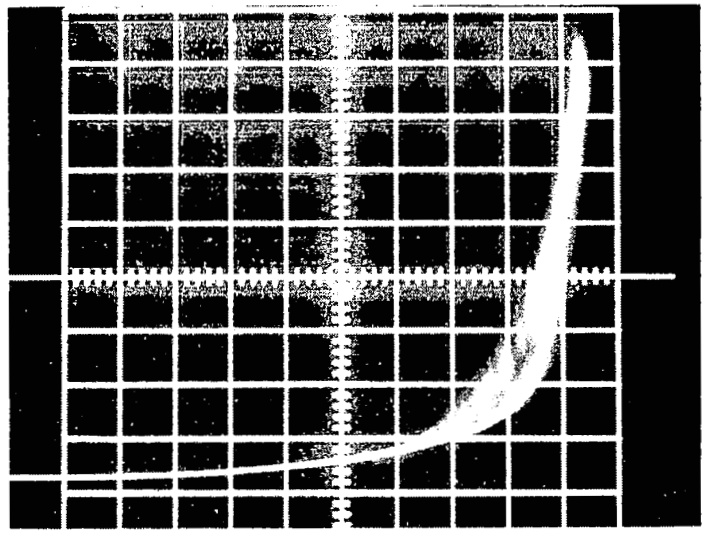

FIGURE 16. I-V FORWARD CHARACTERISTICS SHOWING OSCILLATIONS AT ROOM TEMPERATURE

Scale – Horizontal - 1 volt/division
Vertical - 0.2 ma/division

For rectifiers with a base carrier concentrations $>10^{17}/cm^3$ and with the closed tube zinc vapor diffusion process, the capacity-voltage relation can be satisfied by a square law dependency (i.e. C^{-2} vs. V applied). This suggests an abrupt junction. For example, sample lNA74-029 exhibits such a behavior. The capacity voltage data for samples having lower base carrier levels ($>10^{17}/cm^3$) and/or fabricated by solid-solid diffusion are complex and not readily interpretable (in terms of abrupt or graded junctions).

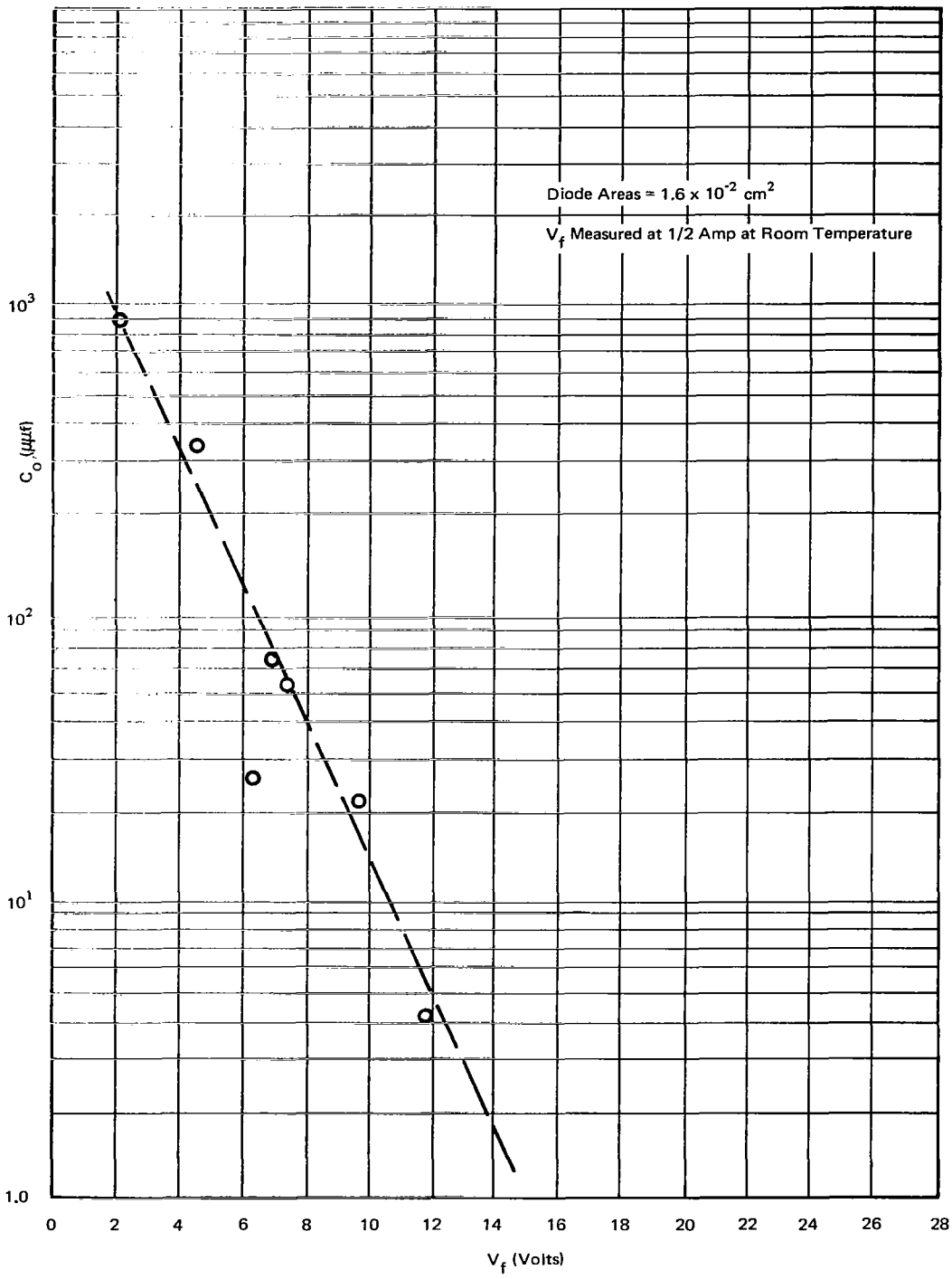

FIGURE 17 ZERO BIAS CAPACITANCE VS. FORWARD VOLTAGE DROP AT 0.5 AMPERES

VII. CONCLUSIONS

Half ampere gallium phosphide rectifiers with current densities of 30 ampere/cm^2 and operate on temperatures up to 400°C have been developed from epitaxially deposited single crystal gallium phosphide.

Best overall characteristics obtained at 400°C are a D. C. reverse voltage of 54 volts (∿75 volts PIV) at 5 ma reverse current. The reverse voltage is somewhat lower than hoped for. These results were obtained by forming p-n junctions using closed tube zinc vapor diffusion.

Using another fabrication approach, namely a solid-solid diffusion process, to fabricate GaP rectifiers, we have been able to make a rectifier which has a D. C. reverse voltage of 175 volts (at 200 μa reverse current) at temperature of 300°C and a D. C. forward voltage drop of 5.7 volts at 0.5 amperes. The room temperature characteristics are 4.6 volts forward drop at 0.5 amperes and 180 volts D. C. reverse voltage with a reverse current of 100 μa. The exact structure has not been determined or the process optimized; although, if it is a p-n junction, the p-layer is very shallow and less than 1/4 micron. It is believed that the structure may be of the metal-insulator-(n) semiconductor type. An interesting aspect of the process is that a negative resistance is found in the forward direction.

The single crystal GaP used to fabricate rectifiers was n-type with room temperature carrier concentrations of mid $10^{16}/cm^3$, 77°K mobility of about 1200 cm^2/volt-sec, and an etch pit density of about 10^6 etch pits/cm^2. The material was grown on GaAs substrates and was grown primarily on the <111>B orientation. The epitaxial material grown was of imperfect structure as evidenced by the high dislocation density. Deep levels such as oxygen were present, and the existence of vacancies was a distinct possibility. Sulfur, nitrogen, oxygen seem to be present in the GaP. The presence of these impurities and the deep levels prevented the reduction of background levels in GaP below about 2 to 3 x $10^{16}/cm^3$; as a consequence reverse voltages of those materials when prepared by standard zinc diffusion were lower than the desired 150 volts PIV.

The addition of a second shallow donor dopant such as tellurium with the sulfur donor appeared to produce material which gave the best overall I-V rectifier characteristics and was the most stable. There was little change in the forward characteristic with temperature to 400°C.

The housings designed for the rectifiers were adequate to handle the thermal problems.

VIII. RECOMMENDATIONS

Even though progress has been made in developing a 400°C gallium phosphide rectifier, further work is required to improve the reverse characteristics at 400°C, to reduce the forward voltage drop, and to improve device stability. In order to achieve these goals the following is recommended:

A. MATERIAL IMPROVEMENT

Basic to device fabrication and performance is the ability to control the structure of the starting material. Strain, vacancies, defects, and dislocations generally give rise to poor control of the diffusant and lead to non-planar and irregular junctions with decoration of faults and dislocation by the zinc diffusant. Present dislocation density of $10^6/cm^2$ should be reduced to $10^4/cm^2$ or even $10^3/cm^2$. With improvement in structure will come better control of impurities and a reduction of background level from 2×10^{16} to mid $10^{15}/cm^3$.

1. Crystal Growth

Two approaches for achieving better structure in the gallium phosphide are vapor epitaxy and liquid epitaxy on bulk grown gallium phosphide substrates.

a. Vapor Epitaxial GaP

Vapor epitaxial growth of gallium phosphide on bulk gallium phosphide substrates will eliminate structural defects due to lattice mismatch. Preliminary work indicates a reduction in dislocation density from 10^6 to 10^4 dislocations/cm^2 for the single crystal GaP grown on bulk GaP substrates. By analogy with epitaxial growth of gallium arsenide, the epitaxial dislocation density should be even lower then the substrate dislocation density. This result can not be achieved by growth on substrates, themselves initially grown epitaxially, because the high dislocation density of the latter simply propagates into the epitaxial layer. Taylor et. al.[13] have demonstrated the dramatic effect, on both room temperature and liquid nitrogen temperature mobilities, of using bulk gallium phosphide substrates. In the latter case one sample attained a liquid nitrogen mobility of over 2,000 cm^2/volt-sec. Optimistically, a parallel improvement in rectifier performance could be attained.

A further advantage of epitaxial growth on gallium phosphide substrates is that, for practical devices, since only a thin layer of active material is required, a much shorter time is required for growth. In addition, by growing the layer on a more highly conducting substrate, the forward resistance of the device can be lowered, permitting higher current carrying capacity.

b. Liquid Epitaxial GaP

The use of liquid epitaxial growth eliminates one potentially serious source of contamination -- the hydrogen chloride gas used in the vapor epitaxial growth technique. Furthermore, an additional purification step may be involved since high purity gallium phosphide previously synthesized at a relatively low temperature from gallium and phosphide can be used to prepare the saturated gallium phosphide solution.

2. Reduction of Impurity Level

A reduction in the background impurity level from 2-3 x 10^{16} to the mid $10^{15}/cm^3$ range should be facilitated by the use of purer and more carefully prepared starting materials.

The improvement in structure and the use of better starting materials should result in improvement of carrier lifetime which should in turn improve forward characteristics (lower forward voltage drop). At the same time the reverse voltage should improve since the background level will be decreased permitting a lower net carrier concentration and higher reverse voltages.

B. INVESTIGATION OF BEST ELECTRICAL STRUCTURE FOR FABRICATION OF HIGH TEMPERATURE RECTIFIERS

An evaluation of junctions with consideration as to the use and control of zinc as a diffusant should be made. Criterion should be I-V characteristics, stability and reversibility of the resultant rectifier. The use of a metal-insulator-semiconductor structure or a Schottky barrier may be considered. The M-S (Schottky barrier) structure has the advantage of completely eliminating zinc but of introducing other problems relating to selection of a metal that will not alloy at high temperatures, that will have suitable and compatible thermal characteristics to the gallium phosphide and will not unduly strain or undergo stress fatigue and crack.

IX. SAMPLES SUBMITTED TO NASA

Rectifier Number	D.C. Forward Voltage Drop, V_f (volts), at 1/2 Ampere at Room Temperature	D.C. Reverse Voltage V_R (volts) at 0.1 ma Reverse Current at Room Temperature
7NA87G21-29-2	8.1	90
3NA87G21-29-2	8.5	78
6NA87G21-29-2	8.3	75
4NA87G21-29-2	10	100
8NA87G21-29-4	10.4	92
1NA80G20-39	5.1	60
2NA79G20-41	5.5	50
2NA87G21-30-3	37	233
5NA76G20-40	4.5	50
2NA77G20-41	2.9	40
1NA77G20-42	3.0	40
3NA76G20-39	5.5	55
5NA76G20-39	8.0	68
1NA81G20-42	4.2	40
2NA76G20-40	3.5	41
4NA76G20-40	4.0	45
5NA87G21-29-2	11.6	89
4NA87G21-30-3	47	251
2NA77G20-42	3.5	35
2R71G20-41	3.5	30
3NA80G20-39	4.3	50
2NA80G20-39	5.6	35
1NA78GP1-4-2	2.99	18
4NA76G20-39	7.3	64
3NA76G20-40	3.5	35
1NA74-029	2.1	12
1NA74GP1-3-1	4.0	23
6NA76G20-39	6.8	60
7NA76G20-39	7.6	64
8NA76G20-39	8.1	54
2NA87G21-30-3	15.8	46
3NA87G21-30-3	30	127
4NA87G21-30-3	16.5	90
5NA87G21-30-3	18.3	83
1NA87G21-29-2	11.3	66
3NA87G21-29-2	9.6	48
3NA77G20-41	3.2	30
6NA76G20-40	4.7	44
8NA76G20-40	4.2	38
4NA77G20-42	3.6	34

Rectifier Number	D.C. Forward Voltage Drop, V_f (volts), at 1/2 Ampere at Room Temperature	D.C. Reverse Voltage V_R (volts) at 0.1 ma Reverse Current at Room Temperature
5NA77G20-42	3.6	30
7NA76G20-40	6.1	33
3NA77G20-42	3.6	26
3NA81G20-41	3.1	21
1NA81GP1-4-2	2.2	20
2NA90G21-30-1	5.9	20
1NA89G21-30-1	4.9	21
1NA78GP1-5-2	2.2	11
3R71G20-41	5.5	20
1NA79G20-39	10.1	23
1NA82GP2-1	4.4	5
2NA81G20-41	2.6	5
3R69G20-38	2.8	5.3

REFERENCES

1. R. E. Davis, "Properties of Elemental and Compound Semiconductors," edited by H. C. Gates, Interscience Publishers, New York, (1960), p. 295.

2. J. Mandelkorn, "Electrical Characteristics of Some Gallium Phosphide Devices," Proc. IRE, 47, 2012-13 (1959).

3. S. M. Sze and G. Gibbons, "Avalanche Breakdown Voltages of Abrupt and Linearly Graded p-n Junctions in Ge, Si, GaAs and GaP", Appl. Phys. Lett. 8, 111 (1966).

4. A. S. Epstein, "Properties of Green Electroluminescence and Double Injection in Epitaxial Gallium Phosphide at Liquid Nitrogen Temperature," Trans. A.I.M.E. 239, 370 (1967).

5. S. J. Bass and P. E. Oliver, "Pulling of Gallium Phosphide Crystals By Liquid Encapsulation," J. Crys. Growth 3, 4, 286 (1968).

6. W. O. Groves, "The Effect of Growth Orientation on the Impurity Content of Epitaxially Grown Gallium Phosphide," Proc. of an International Conference on Crystal Growth, Boston, 20-24, June, 1966, Pergaman Press, New York, (1967), Supplement to J. Phys. Chem. Solids, p. 669.

7. J.A.W. van der Does de Bye and R. C. Peters, "Preparation and Properties of Epitaxial Gallium Phosphide Grown by HCl-Gas Transport, Philips Res. Reports, 24, 210 (1969).

8. P. J. Dean, "Absorption and Luminescence of Excitons at Neutral Donors in Gallium Phosphide, Phys. Rev. 157, 655 (1967).

9. K. G. McKay, "Avalanche Breakdown in Silicon," Phys. Rev. 94, 877 (1954).

10. C. R. Crowell and S. M. Sze, "Temperature Dependence of Avalanche Multiplication in Semiconductors," Appl. Phys. Lett. 9, 242 (1966).

11. S. M. Sze, Physics of Semiconductor Devices, Wiley-Interscience, New York, (1969), chapters 2 and 3.

12. M. Gershenzon and A. Ashkin, "Light Emission Associated with Growth Defects from Reverse Biased GaP p-n Junctions," J. Appl. Phys. 37, 246 (1966).

13. R. A. Logan, H. G. White and F. A. Trumbore, "p-n Junctions in Compensated Solution-Grown GaP," J. Appl. Phys. 38, 2500 (1967).

14. A. S. Epstein, "Room Temperature Green Electroluminescent Diodes Prepared from n-Type Vapor Grown Epitaxial Gallium Phosphide, Solid State Electronics, 12, 485 (1969).

15. R. C. Taylor, J. F. Woods and M. R. Lorenz, "Electrical and Optical Properties of Vapor Grown GaP," J. Appl. Phys. 39, 5404 (1968).

NASA-Langley, 1970 — 9 E-5310